Glutathione Regulates 1-Aminocyclopropane-1-Carboxylate Synthase Transcription via WRKY33 and 1-Aminocyclopropane-1-Carboxylate Oxidase by Modulating Messenger RNA Stability to Induce Ethylene Synthesis during Stress[1][OPEN]

Riddhi Datta, Deepak Kumar, Asma Sultana, Saptarshi Hazra, Dipto Bhattacharyya[2], and Sharmila Chattopadhyay*

Plant Biology Laboratory, Organic and Medicinal Chemistry Division, Council of Scientific and Industrial Research-Indian Institute of Chemical Biology, Kolkata 700 032, India

ORCID IDs: 0000-0001-7490-190X (R.D.); 0000-0002-7739-1025 (A.S.); 0000-0002-8013-7079 (D.B.).

Glutathione (GSH) plays a fundamental role in plant defense-signaling network. Recently, we have established the involvement of GSH with ethylene (ET) to combat environmental stress. However, the mechanism of GSH-ET interplay still remains unexplored. Here, we demonstrate that GSH induces ET biosynthesis by modulating the transcriptional and posttranscriptional regulations of its key enzymes, 1-aminocyclopropane-1-carboxylate synthase (ACS) and 1-aminocyclopropane-1-carboxylate oxidase (ACO). Transgenic Arabidopsis (*Arabidopsis thaliana*) plants with enhanced GSH content (*AtECS*) exhibited remarkable up-regulation of *ACS2*, *ACS6*, and *ACO1* at transcript as well as protein levels, while they were down-regulated in the GSH-depleted *phytoalexin deficient2-1* (*pad2-1*) mutant. We further observed that GSH induced *ACS2* and *ACS6* transcription in a WRKY33-dependent manner, while *ACO1* transcription remained unaffected. On the other hand, the messenger RNA stability for *ACO1* was found to be increased by GSH, which explains our above observations. In addition, we also identified the ACO1 protein to be a subject for *S*-glutathionylation, which is consistent with our in silico data. However, *S*-glutathionylation of ACS2 and ACS6 proteins was not detected. Further, the *AtECS* plants exhibited resistance to necrotrophic infection and salt stress, while the *pad2-1* mutant was sensitive. Exogenously applied GSH could improve stress tolerance in wild-type plants but not in the ET-signaling mutant *ethylene insensitive2-1*, indicating that GSH-mediated resistance to these stresses occurs via an ET-mediated pathway. Together, our investigation reveals a dual-level regulation of ET biosynthesis by GSH during stress.

Plants are sessile organisms and are continuously threatened by a range of biotic and abiotic stress factors. Consequently, they have evolved highly sophisticated defense strategies to efficiently sense, respond, and adapt to their ever-changing environment and ensure survival. The significance of salicylic acid (SA), jasmonic acid (JA), and ethylene (ET) as primary signal molecules in the regulation of plant defense response has been well documented (Dong, 1998; Thomma et al., 1998; van Loon et al., 2006; Loake and Grant, 2007). Over the past 2 decades, the critical role of glutathione (GSH) during stress has also been reported (Noctor et al., 2012). In plants, SA-mediated signaling pathway operates during defense against biotrophic infection, while the defense against necrotrophic infection is regulated by JA- and ET-mediated pathways (Glazebrook, 2005; Stout et al., 2006). Extensive crosstalk between these three pathways, along with other signaling molecules, provides the plant with powerful strategies to fine-tune its defense response (Reymond and Farmer, 1998; Kunkel and Brooks, 2002; Pieterse and Dicke, 2007).

One of the simplest phytohormones is ET. It regulates a broad spectrum of developmental and physiological processes, including germination, growth, senescence, ripening, and responses to biotic and abiotic stresses (Abeles et al., 1992; Etheridge et al., 2005; Shakeel et al., 2013). The importance of ET in regulating the plant

[1] This work was supported by the Department of Science and Technology, New Delhi, India; the Council of Scientific and Industrial Research, New Delhi, India; and fellowships from the Indian Council of Medical Research (to R.D.), the Council of Scientific and Industrial Research (to D.K.), the Department of Science and Technology (to A.S.), and the University Grant Commission (to S.H.).

[2] Present address: Division of Biotechnology, Chonbuk National University, 79 Gobong-ro, Iksan-si, Jeollabuk-do 570–752, Republic of Korea.

* Address correspondence to sharmila@iicb.res.in.

The author responsible for distribution of materials integral to the findings presented in this article in accordance with the policy described in the Instructions for Authors (www.plantphysiol.org) is: Sharmila Chattopadhyay (sharmila@iicb.res.in).

S.C. and R.D. conceived and designed the original research plans; R.D. performed most of the experiments; D.K. performed the cloning experiments and helped R.D. during other experiments; R.D., D.K., A.S., S.H., and D.B. analyzed the data; R.D. wrote the article. with contributions of all the authors; S.C. supervised and complemented the writing.

[OPEN] Articles can be viewed without a subscription.

www.plantphysiol.org/cgi/doi/10.1104/pp.15.01543

response to biotic and abiotic stresses such as those induced by pathogen infection, flooding, salt, or drought has been well documented (O'Donnell et al., 1996, 2003; Penninckx et al., 1998; Cao et al., 2007). ET production by infected plants is an early resistance response leading to activation of plant defense, and it affects both the plant and the pathogen (Chagué et al., 2006). It activates the plant defense-related processes such as production of phytoalexins (Fan et al., 2000), induction of the phenylpropanoid pathway (Chappell et al., 1984), and cell wall alterations (Bell, 1981). Exogenously applied ET has also been reported to induce resistance in many host-pathogen interactions studied (Esquerré-Tugayé et al., 1979; Elad, 1990; Marte et al., 1993). The study of various ET mutants in Arabidopsis (*Arabidopsis thaliana*), tobacco (*Nicotiana tabacum*), and soybean (*Glycine max*) have revealed that ET signaling is required for resistance against some specific pathogens such as *Botrytis cinerea*, but not to others (Knoester et al., 1998; Hoffman et al., 1999). ET has also been reported to play a crucial role in salt, drought, and heat stress tolerance by gene-specific regulations, where the ethylene response factor1 (ERF1) plays a nodal role integrating the ET- and JA-signaling pathways (Cheng et al., 2013). Salt stress induces ET biosynthesis; the ET may then inhibit its receptors, suppress salt sensitivity conferred by ET receptors, and promote ET-responsive salt tolerance (Achard et al., 2006; Cao et al., 2007). ET has also been documented to provide protection against heat stress-induced oxidative damage along with calcium, abscisic acid, and SA (Larkindale and Knight, 2002). On the other hand, overexpression of Hahb-4, a transcriptional repressor of ET synthesis, has been reported to significantly increase desiccation tolerance in Arabidopsis (Manavella et al., 2006). Similarly, suppression of ET synthesis in maize (*Zea mays*) could improve grain yield under drought stress condition (Habben et al., 2014). This extensive involvement of ET in various aspects of plant life has made it a focus of intense research for decades. Even though many components of its biosynthesis and signaling pathways have already been deciphered, much remains to be learned about the pathways and the complex regulation of the genes and proteins involved (Chen et al., 2005).

However, unlike the overwhelming amount of evidences demonstrating the crosstalk among SA, JA, and ET in plant defense, the role of GSH in this cross-communication network is less well understood. This tripetide thiol performs many important functions in plant, including antioxidant defense and redox signaling (Foyer and Noctor, 2011; Noctor et al., 2012). In addition to this central task, the potential role of GSH in cellular defense is also well recognized for the last 3 decades (Dron et al., 1988; Wingate et al., 1988; Bradley et al., 1992). The unique structural properties, abundance, redox potential, and wide distribution in most living organisms have drawn momentous attention toward this molecule (Meister, 1988; May et al., 1998).

Previous studies have demonstrated that enhanced GSH level can significantly induce tolerance against various environmental stress conditions (Noctor et al., 1998; Zhu et al., 1999; Gullner et al., 2001; Gomez et al.,

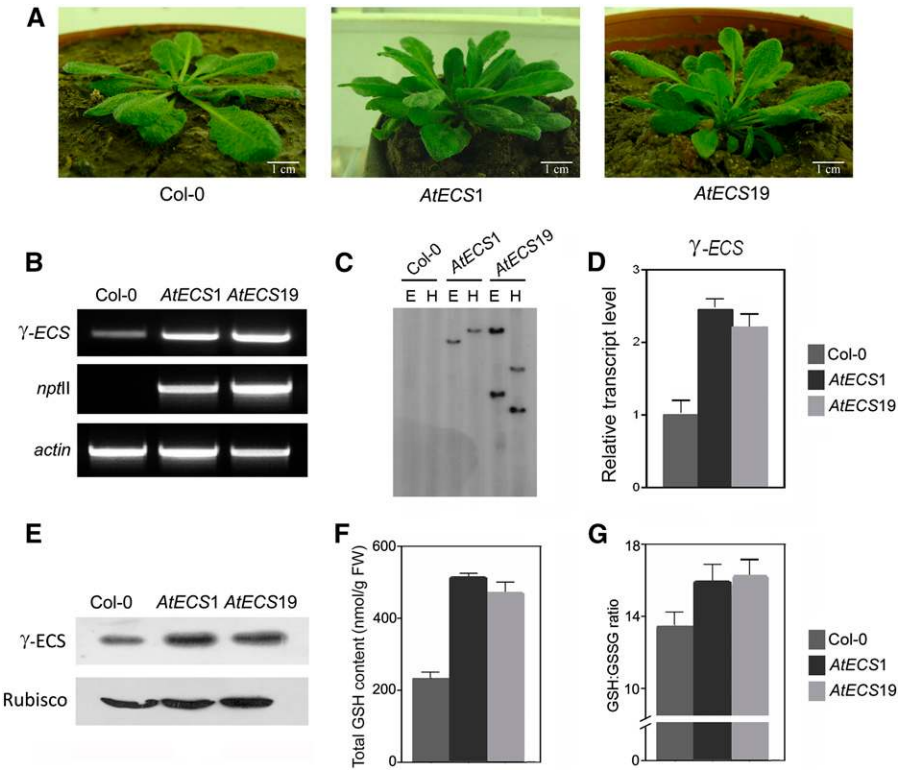

Figure 1. Characterization of T4 generation *AtECS* lines. Leaves from 4-week-old plants grown in growth chamber were used for analysis. A, Four-week-old Col-0, *AtECS1*, and *AtECS19* plants. B, Genomic DNA PCR screening of *γ-ECS* and *npt*II genes in *AtECS* lines. C, Southern-blot analysis of *AtECS* lines for the transgene integration. Single copy insertion of the transgene was detected in *AtECS1*, while two copies were detected in *AtECS19*. D, qRT-PCR analysis for *γ-ECS* gene expression in *AtECS* lines. The relative transcript abundance was found to be more than 2-fold higher in *AtECS* lines compared with Col-0. E, Western-blot analysis of *AtECS* lines showing γ-ECS protein overexpression. F, Total GSH content estimation by HPLC analysis. GSH content was found to be 2.24- and 1.92-fold higher in *AtECS1* and *AtECS19*, respectively, compared with Col-0. G, Estimation of GSH:oxydized GSH (GSSG) ratio in *AtECS* lines. All experiments were repeated three times. FW, Fresh weight; E, *Eco*RI; H, *Hin*dIII.

2004; Mullineaux and Rausch, 2005; Liedschulte et al., 2010). Transgenic Arabidopsis plants with low GSH level (10% of the wild type) exhibit hypersensitivity to cadmium stress due to the limited capacity of these plants to make phytochelatins (Xiang et al., 2001). Loss-of-function analysis has also been widely employed for defining the biological roles of GSH in plants. Considering all its vital functions, a null mutation is likely lethal, and no such mutants has been reported yet. The *cadmium sensitive2-1* mutant of Arabidopsis produces GSH at a level of 30% of the wild type and is hypersensitive to some toxic metals (Howden et al., 1995). The *phytoalexin deficient2-1* (*pad2-1*) mutant, with only 22% of GSH found in wild-type plants, has been reported to be deficient in camalexin (Glazebrook and Ausubel, 1994; Parisy et al., 2007). Another GSH mutant, the *root meristemless1*, contains only 3% GSH and exhibits a root meristem-less phenotype (Vernoux et al., 2000). All these GSH-deficient mutants have compromised resistance to both microorganisms and insects (Ball et al., 2004; Parisy et al., 2007; Schlaeppi et al., 2008; Datta and Chattopadhyay, 2015).

The involvement of GSH with other defense-signaling pathways has also been documented. The addition of GSH has been reported to mimic SA in inducing *pathogenesis-related protein1* (*PR1*), possibly through *nonexpressor of pathogenesis-related genes1* (*NPR1*) reduction and relocation to the nucleus (Mou et al., 2003; Gomez et al., 2004). Our previous investigation revealed that GSH mitigates biotic stress in plants through NPR1-dependent SA-mediated pathway (Ghanta et al., 2011a, 2011b; Ghanta and Chattopadhyay, 2011). However, it appears that the influence of GSH on biotic stress signaling extends beyond that mediated through the NPR1 function. Later on, it has been noted that GSH may also act through NPR1-independent pathway to increase intracellular hydrogen peroxide, which activates SA signaling (Han et al., 2013). Only very recently, we have reported that an enhanced GSH level can provide resistance against *B. cinerea* infection, presumably through its crosstalk with ET (Ghanta et al., 2014). However, the mechanism of this GSH-ET interplay is still unexplored. In this investigation, we aimed to dissect the molecular mechanism of the GSH-ET interaction during stress. Our results demonstrate that GSH induces ET biosynthesis via transcriptional as well as posttranslational regulations.

RESULTS

Raising Transgenic Arabidopsis with Enhanced GSH Content (*AtECS*)

The enzyme γ-glutamyl-cysteine synthetase (γ-ECS; EC 6.3.2.2) catalyzes the rate-limiting step of GSH biosynthesis (Hell and Bergmann, 1990; May et al., 1998). Here, we have cloned the *Lycopersicum esculentum*

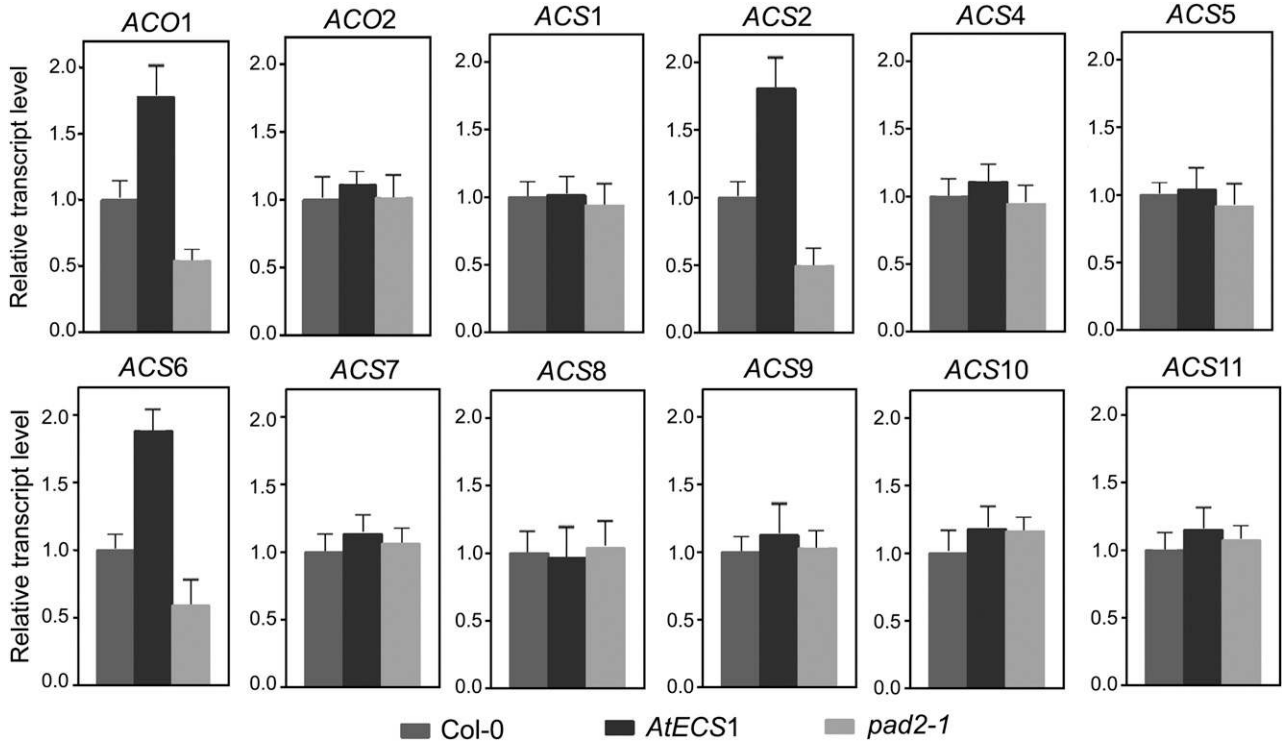

Figure 2. Effect of altered GSH levels on the transcript levels of various isoforms of *ACS* and *ACO* genes. Leaves from 4-week-old Col-0, *AtECS1*, and *pad2-1* plants were used for qRT-PCR analysis using *actin* as the reference gene. Significant alteration in transcript level was observed in case of *ACO1*, *ACS2*, and *ACS6* genes. Data are the mean ± SD for three individual experiments using plants grown independently.

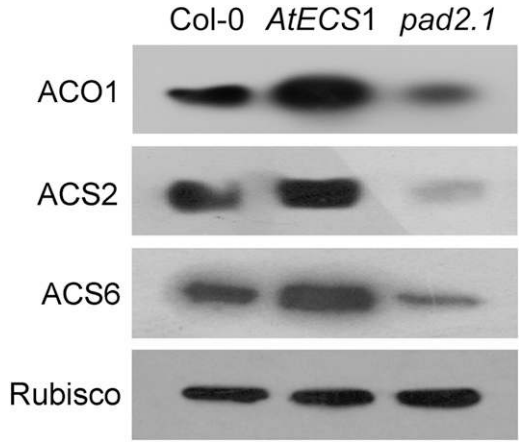

Figure 3. Effect of altered GSH levels on ACS and ACO proteins. Western-blot analysis for ACS2, ACS6, and ACO1 was performed using the leaves of 4-week-old Col-0, *AtECS1*, and *pad2-1* plants. All three proteins were up-regulated in *AtECS1* while down-regulated in *pad2-1*. Experiments were performed in replicates of three.

γ-ECS gene into a pBI121 vector under the control of the *Cauliflower mosaic virus 35S* (*CaMV35S*) constitutive promoter as described before (Ghanta et al., 2011a). The resulting $P_{CaMV35S}$:*Leγ-ECS* construct was used to transform ecotype Columbia (Col-0) plants following standard floral dip method (Clough and Bent, 1998). After transformation, two independent transgenic lines (*AtECS1* and *AtECS19*) were selected, and homozygous plants were obtained using kanamycin resistance and were confirmed to carry the complete construct by PCR. No notable morphological differences were observed between Col-0 and *AtECS* plants except petiole hyponasty (Fig. 1A), which is an ET-driven adaptive response in plants (Polko et al., 2011). We further characterized the *AtECS1* and *AtECS19* lines by Southern-blot, quantitative reverse transcription (qRT)-PCR, and western-blot analyses for the transgene expression (Fig. 1, B–G; Supplemental Fig. S1). The GSH content was found to be 2.24- and 1.92-fold higher in *AtECS1* and *AtECS19*, respectively, compared with Col-0 (Fig. 1F). The *AtECS1* line with higher *γ-ECS* expression and GSH content was used for further analyses.

Comparative Proteome Analysis Revealed Up-Regulation of ACO in *AtECS1*

To investigate the effect of the altered GSH level on cellular protein, we analyzed the differential protein abundance in *AtECS1*, Col-0, and *pad2-1* leaves using two-dimensional gel electrophoresis coupled to matrix-assisted laser desorption/ionization (MALDI)-time of flight (TOF)-tandem mass spectroscopy (MS/MS) as standardized previously (Sinha et al., 2014). Supplemental Figure S2A shows the representative images of *AtECS1*, Col-0, and *pad2-1* gels. The number of resolved spots was 294, 277, and 289 in *AtECS1*, Col-0, and *pad2-1* gels, among which 71 differentially expressed spots were identified (Supplemental Tables S1 and S2). The overall mean coefficient of variation of the spots matched was determined to be 38.46%. Functional classification revealed that 51% of the identified proteins belonged to stress and defense category, 38% to carbon and energy metabolism, and 11% to others category (Supplemental Fig. S2B).

Among the identified proteins, 1-aminocyclopropane-1-carboxylate (ACC) oxidase (ACO), which catalyzes a key step in ET biosynthesis, was found to be up-regulated in *AtECS1* and down-regulated in *pad2-1*. This observation, together with our previous report (Ghanta et al., 2014), suggests an induction of ET biosynthesis by GSH.

ASC2, ACS6, and ACO1 Expressions Are Induced at the Transcript and Protein Levels under Enhanced GSH Conditions

ET biosynthesis is a two-step process where the first step is catalyzed by ACC synthase (ACS) and the final step is catalyzed by ACO. To further investigate the

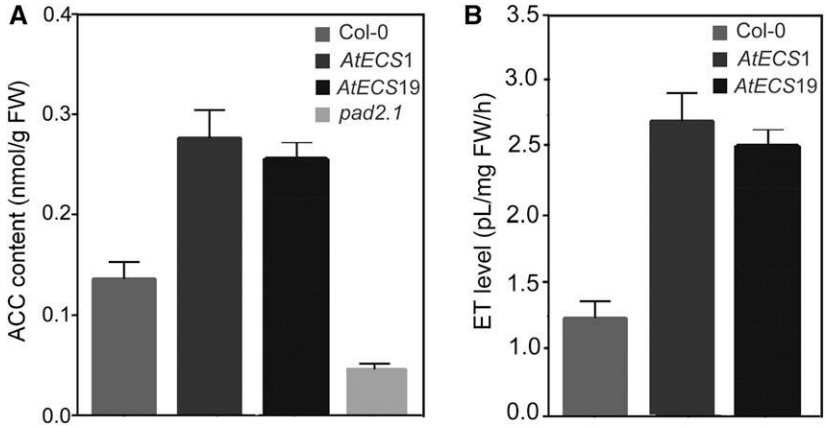

Figure 4. Effect of altered GSH levels on ACC and ET contents. A, ACC content was estimated by HPLC analysis from leaves of 4-week-old Col-0, *AtECS1*, *AtECS19*, and *pad2-1* plants. The ACC content was found to be 1.9-fold in *AtECS1*, 1.83-fold in *AtECS19*, and 0.46-fold in *pad2-1* compared with Col-0. B, ET level was estimated from leaves of 4-week-old Col-0, *AtECS1* and *AtECS19* plants. The ET levels were found to be 2.1-fold in *AtECS1* and 1.96-fold in *AtECS19* compared with Col-0. Data are the mean ± SD for three individual experiments using plants grown independently. FW, Fresh weight.

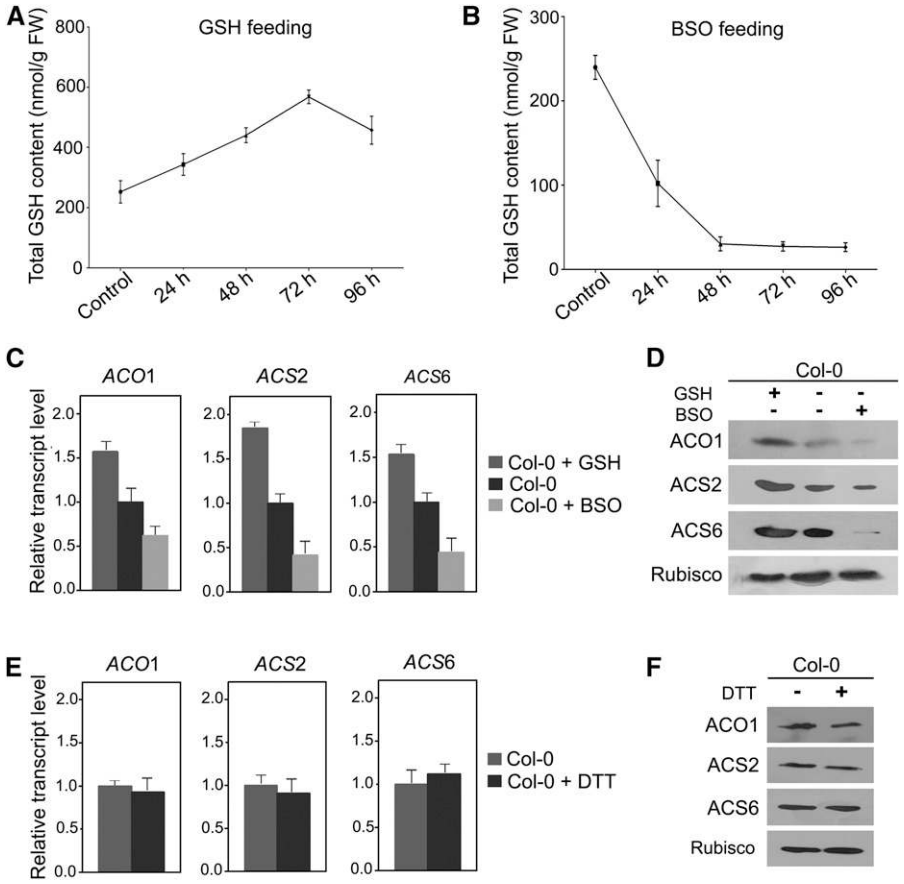

Figure 5. Effect of GSH, BSO, and DTT feeding on the expression of ACS and ACO. Two-week-old Col-0 plants were fed with 100 μM GSH (A) and 1 mM BSO (B), and leaf GSH content was estimated by HPLC analysis on a temporal landscape. A 72-h feeding was found to be optimum in both cases. Expression profiles of *ACO1*, *ACS2*, and *ACS6* genes (C) and proteins (D) in GSH- and BSO-fed Col-0. *ACO1*, *ACS2*, and *ACS6* were significantly up-regulated in GSH-fed plants while down-regulated in BSO-fed plants at transcript as well as protein levels. Effect of DTT feeding on the expression levels of *ACO1*, *ACS2*, and *ACS6* genes (E) and proteins (F). No significant alteration in their expression levels was observed. All experiments were repeated three times. FW, Fresh weight.

effect of GSH on ET biosynthesis, we studied various isoforms of *ACS* and *ACO* genes reported in Arabidopsis genome. The qRT-PCR analysis revealed that expression of *ACS2*, *ACS6*, and *ACO1* genes were remarkably up-regulated in *AtECS1* and down-regulated in *pad2-1*, while the rest of the isoforms were unaffected (Fig. 2). A higher abundance of ACS2, ACS6, and ACO1 proteins in *AtECS1* and lower abundance in *pad2-1* was also revealed by western-blot analysis (Fig. 3). HPLC analysis demonstrated that ACC contents in *AtECS1* and *AtECS19* were 1.9- and 1.82-fold higher than Col-0 while lower in *pad2-1* by 0.46-fold (Fig. 4A). ET content was also found to be 2.1-fold in *AtECS1* and 1.96-fold in *AtECS19* compared with Col-0 (Fig. 4B).

Next, we fed Col-0 plants with exogenous GSH and a GSH inhibitor, buthionine sulphoximine (BSO). Estimation of GSH content by HPLC analysis was used to monitor the GSH- and BSO-fed plants. A 72-h treatment was found to be optimum in both cases and selected for further analyses (Fig. 5, A and B). The expression of *ACS2*, *ACS6*, and *ACO1* genes were found to be up-regulated in GSH-fed plants and down-regulated in BSO-fed plants compared with control (Fig. 5C). Western-blot analysis further confirmed higher abundance of ACS2, ACS6, and ACO1 proteins in GSH-fed plants and their lower abundance in BSO-fed plants (Fig. 5D). These observations strongly suggest that GSH induces ET biosynthesis by regulating ACS2, ACS6, and ACO1. ET levels were also enhanced in the GSH-fed plants (Supplemental Fig. S3).

To examine if this GSH-mediated regulation of ET biosynthesis is a secondary effect due to changes in redox homeostasis, we fed Col-0 plants with two separate reducing agents (dithiothreitol [DTT] and β-mercaptoethanol). Although DTT and β-mercaptoethanol feedings could induce *PR1* (marker gene) gene expression (Supplemental Fig. S4, A and B), it failed to alter the expressions of ACS2, ACS6, and ACO1 at both transcript and protein levels (Fig. 5, E and F; Supplemental Fig. S4B), indicating that the observed up-regulation is not a secondary effect of disturbed redox homeostasis.

GSH Induces Transcription of *ACS2* and *ACS6* But Not *ACO1*

With a view to investigate the effect of GSH on the transcriptional regulation of *ACS2*, *ACS6*, and *ACO1* genes, we have fused these three promoters (i.e., an intergenic region of 1.5 kb upstream from the translation start site) to the *GUS* (*β-glucuronidase*)-*GFP* (*uidA*) reporter genes. The resulting constructs (P_{ACS2}:*GUS-GFP*, P_{ACS6}:*GUS-GFP*, and P_{ACO1}:*GUS-GFP*) were stably

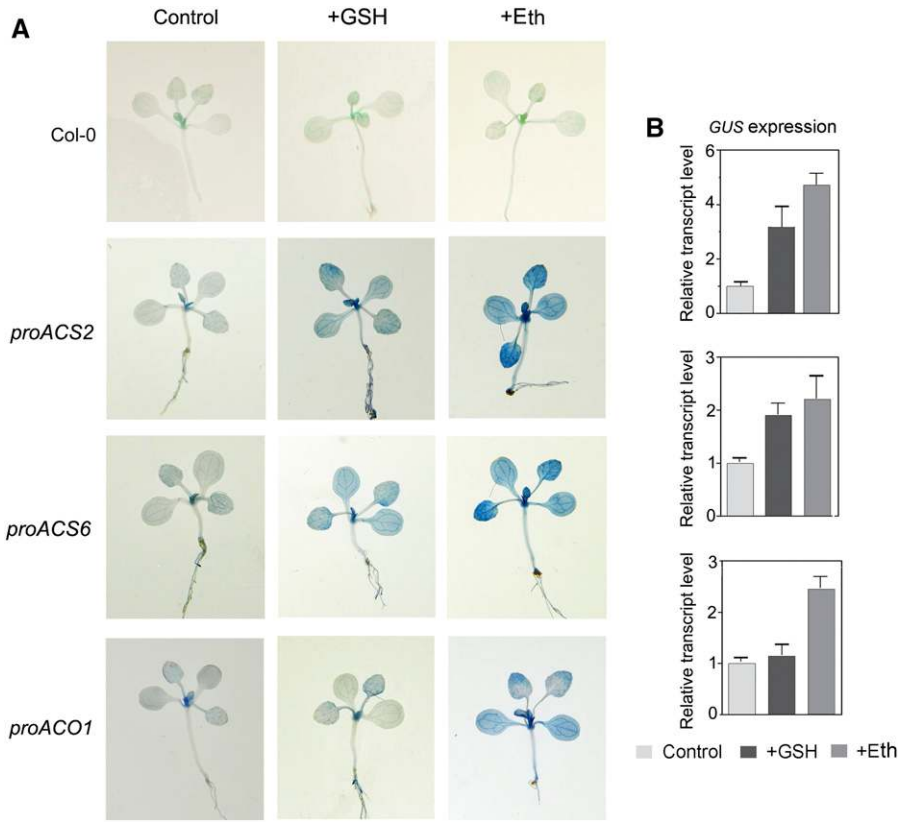

Figure 6. Analysis of promoter activity of *proACS2*, *proACS6*, and *proACO1* in response to GSH and Eth feeding. A, GUS activity assay. B, Expression levels of *GUS* gene by qRT-PCR analysis. Promoter activity was enhanced in case of *proACS2* and *proACS6* in response to GSH feeding, while *proACO1* was unaffected. Eth feeding, on the other hand, increased the activity of all three promoters. All experiments were repeated three times.

introduced into Col-0 plants. A comparative GUS analysis revealed that the *ACS2* and *ACS6* promoter activities were strongly enhanced in response to GSH as well as ethephon (Eth) feeding. On the other hand, the activity of *ACO1* promoter was unaffected by GSH feeding, but its activity increased significantly on Eth feeding (Fig. 6A). The qRT-PCR analysis also indicated a similar pattern of *GUS* gene expression (Fig. 6B). Together, these observations suggest that GSH increases the promoter activity of *ACS2* and *ACS6* but not *ACO1* genes thus up-regulating their transcription. In addition, a positive feedback induction by ET (released by Eth) operates for all the three promoters.

Next, we transfected the P_{ACS2}:*GUS-GFP*, P_{ACS6}:*GUS-GFP*, and P_{ACO1}:*GUS-GFP* constructs into the Col-0 and *AtECS1* protoplasts and monitored their GFP expression levels. Results revealed a higher level of GFP expression in *AtECS1* protoplasts transfected with P_{ACS2}:*GUS-GFP* and P_{ACS6}:*GUS-GFP* compared with the Col-0 protoplasts transfected with the same construct. However, in case of P_{ACO1}:*GUS-GFP*, no significant difference in the GFP expression level of Col-0 and *AtECS1* protoplast was observed (Fig. 7). These observations further support the GSH-mediated induction of the *ACS2* and *ACS6* promoter activities, while the *ACO1* promoter remains unaffected.

WRKY33 Is Essential for GSH-Mediated Transcriptional Induction of *ACS2* and *ACS6*

Because GSH cannot directly modulate promoter activity, it becomes necessary to find out through which pathway this regulation occurs. ACS2 and ACS6 belong to the type I group of ACS isoforms, and their regulation is known to occur via a Mitogen-activated protein kinase kinase4 (MKK4)/MKK5/MKK9-Mitogen-activated protein kinase3 (MPK3)/MPK6 pathway (Li et al., 2012). To check if GSH-mediated transcriptional regulation occurs through this MPK3/MPK6 pathway, we analyzed *ACS2* and *ACS6* expressions in *mpk3* and *mpk6* mutants. It was observed that *ACS2* and *ACS6* expression was severely diminished in the mutants compared with Col-0. However, their expression was still induced in both the mutants in response to *B. cinerea* infection as well as salt stress, which can be corroborated with previous reports (Li et al., 2012). This suggests that even in the absence of MPK3 and MPK6, some alternative pathway operates to induce ET synthesis during stress. We further observed that the *ACS2* and *ACS6* expression levels were up-regulated in both *mpk3* and *mpk6* mutants in response to GSH feeding (Fig. 8A). This was further supported by the observation that *MPK3*, *MPK6*, *MKK4*, *MKK5*, and *MKK9* gene expressions were also unaltered in *AtECS1*, Col-0, and

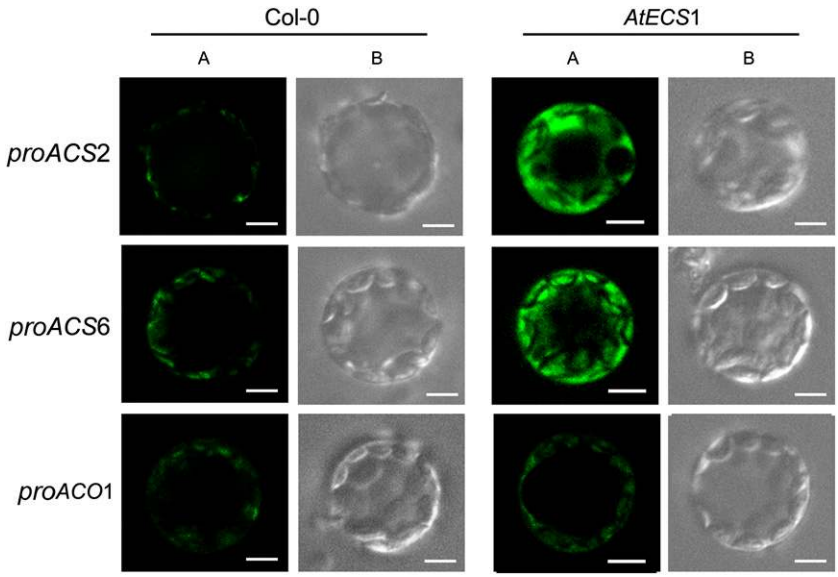

Figure 7. Analysis of promoter activity of *proACS2*, *proACS6*, and *proACO1* in Col-0 and *AtECS1* protoplasts. Leaf protoplasts of Col-0 and *AtECS1* were transfected with P_{ACS2}:*GUS-GFP*, P_{ACS6}:*GUS-GFP*, and P_{ACO1}:*GUS-GFP* constructs, and GFP expression levels were monitored under confocal laser scanning microscope. A, Fluorescence under 488 nm. B, Bright-field image. Higher *GFP* expression was observed in *AtECS1* protoplasts transfected with P_{ACS2}:*GUS-GFP* and P_{ACS6}:*GUS-GFP* constructs compared with Col-0. Experiments were performed in replicates of three. Bar = 10 μm.

pad2-1, indicating that the GSH-mediated induction of *ACS2* and *ACS6* does not involve the MKK4/MKK5/MKK9-MPK3/MPK6 pathway (Supplemental Fig. S5).

Participation of several transcription factors in *ACS2* and *ACS6* regulation is reported. These are WRKY6, WRKY8, WRKY33, WRKY53, ERF4, and ERF11. To check if GSH-mediated transcription induction occurs through these transcription factors, we have checked for *ACS2* and *ACS6* expression levels in these mutants. Although expression levels were diminished in all the mutants, transcriptional induction of *ACS2* and *ACS6* occurred on GSH feeding in *wrky6*, *wrky8*, *wrky53*, *erf4*, and *erf11* mutants. Transcriptional induction of *ACS2* and *ACS6* genes was also noted in response to *B. cinerea* infection and salt stress in all these mutants (Fig. 8B). Together it indicates that GSH-mediated regulation does not occur through these transcription factors. The WRKY33 transcription factor functions downstream of the MKK4/MKK5/MKK9-MPK3/MPK6 pathway and regulates *ACS* gene expression. In the case of the *wrky33* mutant, *ACS2* and *ACS6* expression was not altered in response to GSH feeding as well as *B. cinerea* infection and salt stress (Fig. 8B). This strongly suggests that WRKY33 plays a crucial role in *ACS2* and *ACS6* regulation and that WRKY33 is essential for the GSH-mediated transcriptional regulation of the two genes. In addition to *ACS2* and *ACS6*, *ACO1* expression levels were also checked in all these mutants as another control gene. As expected, the expression of the *ACO1* gene was not significantly altered in these mutants (Supplemental Fig. S6).

These observations prompted us to perform cotransfection assay in *wrky33* mutant protoplasts. We observed that when only the construct, P_{ACS2}:*GUS-GFP* or P_{ACS6}:*GUS-GFP*, was transfected in *wrky33* protoplasts, no GFP fluorescence was detected. Even on treating the transfected protoplasts with GSH, no GFP fluorescence could be detected. We cloned the *WRKY33* gene in the pAMPAT-YFP vector under the control of *CaMV35S* promoter. The resulting construct was $P_{CaMV35S}$:*YFP-WRKY33*. Transfecting this construct in *wrky33* protoplasts restored the WRKY33 expression in the mutant, which was evident from the YFP fluorescence. We cotransfected the construct $P_{CaMV35S}$:*YFP-WRKY33* with P_{ACS2}:*GUS-GFP* or P_{ACS6}:*GUS-GFP* in the *wrky33* protoplast. The GFP expression was restored in the cotransfected protoplasts, reflecting that WRKY33 is essential for *ACS2* and *ACS6* transcription. When these cotransfected protoplasts were treated with GSH, the GFP expression level was enhanced (Fig. 9). Together, these observations confirmed that GSH-mediated induction of *ACS2* and *ACS6* transcription occurs in a WRKY33-dependent manner.

GSH Enhances the Binding of WRKY33 to the *ACS2* and *ACS6* Promoters

To obtain a deeper insight, we performed Chromatin Immunoprecipitation (ChIP)-quantitative PCR (qPCR) analysis for WRKY33 on the *ACS2* and *ACS6* promoters. Interestingly, we observed that the percentage input for *ACS2* and *ACS6* promoters was 7.2 and 6.79 in *AtECS1* compared with 3.6 and 3.52 in Col-0, respectively (Fig. 10). *AtECS19* also displayed a comparable result (Supplemental Fig. S7). Binding of RNA polymerase II to the *glyceraldehyde-3-phosphate dehydrogenase* (*GAPDH*) promoter was used as a control. The percentage input in this case was 3.94 and 3.43 in Col-0 and *AtECS1*, respectively. These results suggest that the higher GSH

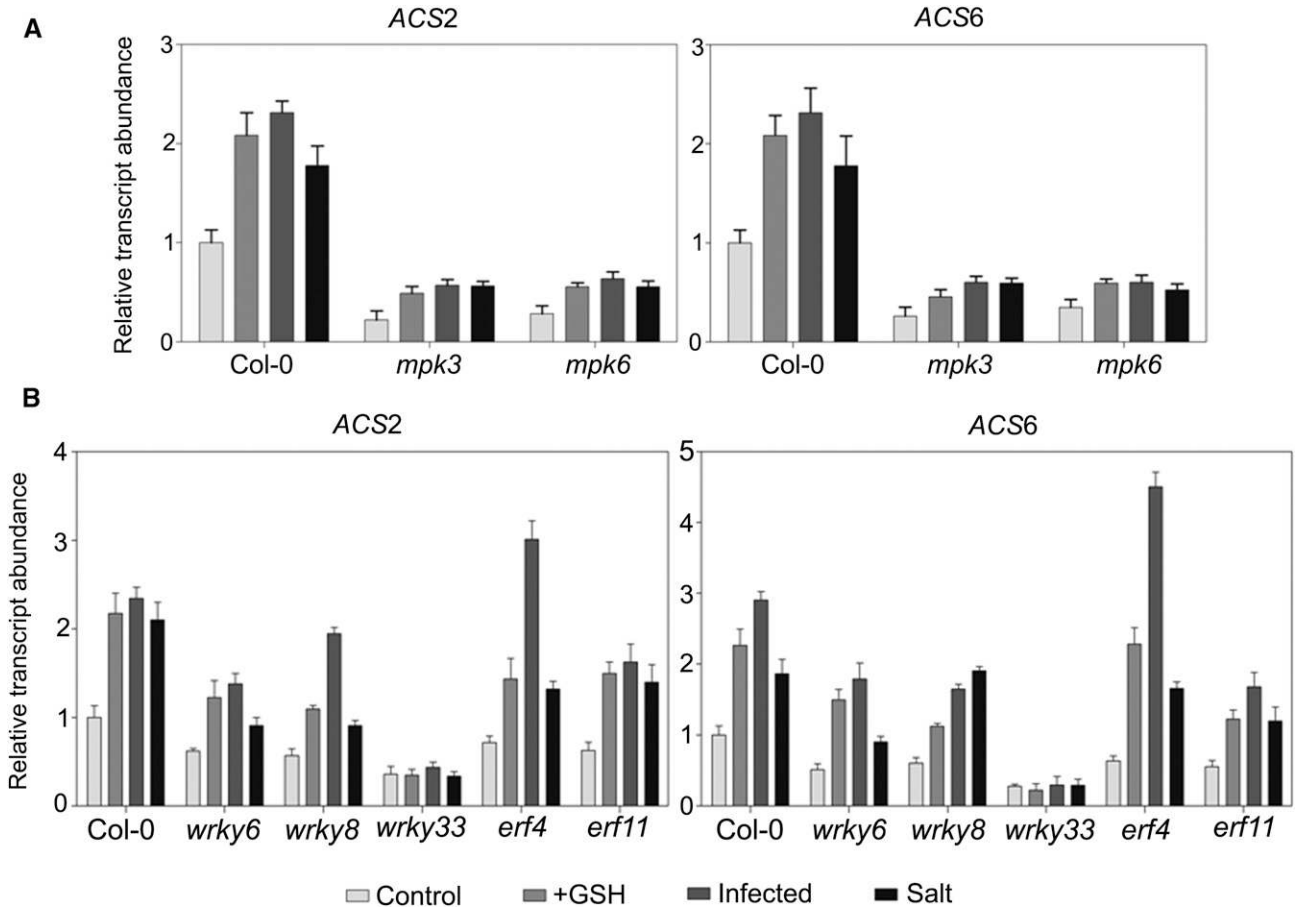

Figure 8. Expression profiles of *ACS2* and *ACS6* genes in *mpk3* and *mpk6* mutants (A) and *wrky6*, *wrky8*, *wrky33*, *erf4*, and *erf11* mutants (B). qRT-PCR analysis was performed in response to GSH feeding, *B. cinerea* infection, and salt stress. No significant alteration in the expression levels of *ACS2* and *ACS6* was observed in case of *wrky33* mutant. Data are the mean ± SD for three individual experiments using plants grown independently.

level in *AtECS1* increased the binding of WRKY33 to the *ACS2* and *ACS6* promoters, thus facilitating transcription of the respective genes.

GSH-Mediated ACO1 Regulation Is Not Due to Ascorbate Limitation

Ascorbate is one of the substrates required for ET synthesis. Ascorbate limitation can be a consequence of GSH depletion and can lead to a lower ET synthesis. To check this, we estimated the ascorbate levels in Col-0, *AtECS* lines, and *pad2-1* mutant (Supplemental Fig. S8). Next, we fed *pad2-1* mutants with ascorbate and GSH separately. ACC content was increased in *pad2-1* mutant in response to GSH feeding but was unaffected by ascorbate feeding. qRT-PCR and western-blot analyses also revealed that ascorbate feeding failed to increase ACO1 transcript and protein abundance in *pad2-1* mutant (Supplemental Fig. S9). This demonstrates that ascorbate limitation is not responsible for lower ET level in *pad2-1* mutant.

GSH Enhances the mRNA Stability of *ACO1*

Because up-regulation of *ACO1* expression was observed at transcript level, but the promoter activity was not affected, we investigated the mRNA stability for *ACO1* in Col-0, *AtECS1*, and *pad2-1*. For that, the Col-0, *AtECS1*, and *pad2-1* seedlings were treated with actinomycin D on a temporal landscape followed by qRT-PCR analysis. Interestingly, we noted that the *ACO1* mRNA stability was considerably increased in *AtECS1*, with a half-life of 6.32 h compared with 6.03 h in Col-0. *AtECS19* also displayed a similar trend (Supplemental Fig. S10). On the other hand, half-life for *ACO1* mRNA in *pad2-1* was found to be 5.76 h (Fig. 11). This result demonstrates that GSH plays a role in maintaining the mRNA stability for *ACO1*.

ACO1 Protein Is a Target for *S*-Glutathionylation

We also checked if ACS and ACO proteins can be subjected to *S*-glutathionylation. Isolation of in vitro

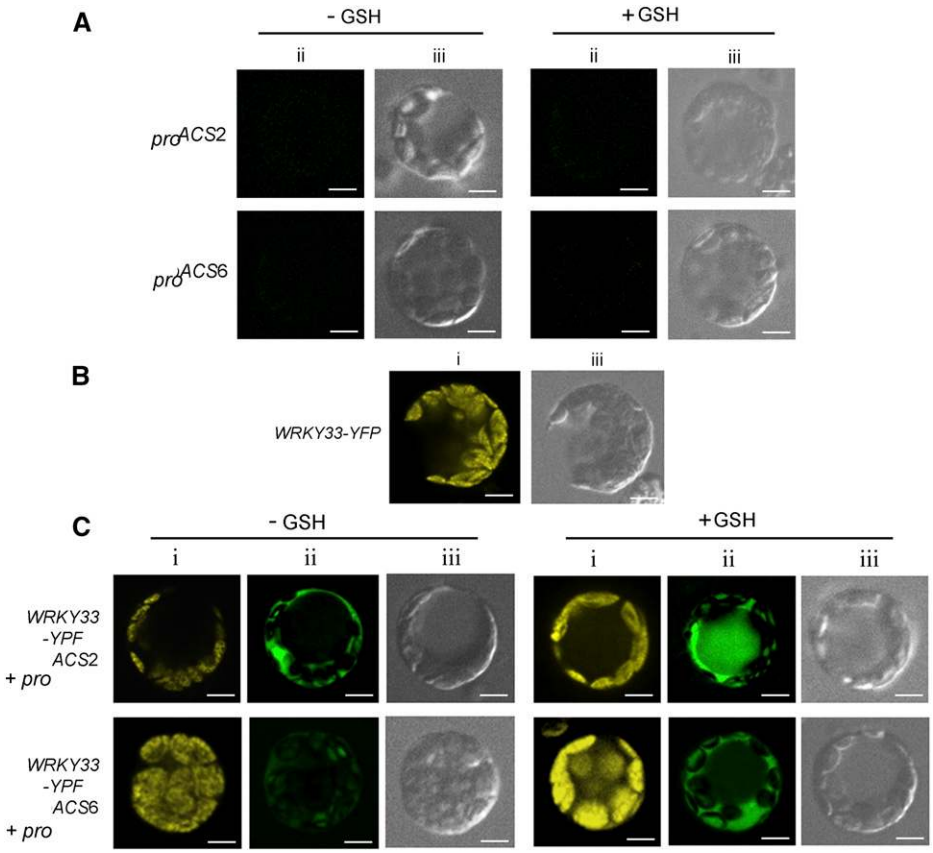

Figure 9. Analysis of promoter activity of *proACS2* and *proACS6* in *wrky33* protoplasts. A, Leaf protoplasts of *wrky33* were transfected with P_{ACS2}:*GUS-GFP* and P_{ACS6}:*GUS-GFP* constructs, and GFP expression levels were monitored under a confocal laser scanning microscope with or without GSH treatment. B, Leaf protoplasts of *wrky33* were transfected with $P_{CaMV35S}$:*YFP-WRKY33* construct, and YFP expression level was monitored under confocal laser scanning microscope. C, Leaf protoplasts of *wrky33* were cotransfected with $P_{CaMV35S}$:*YFP-WRKY33* and P_{ACS2}:*GUS-GFP* or P_{ACS6}:*GUS-GFP* constructs. YFP and GFP expression levels were monitored under confocal laser scanning microscope with or without GSH treatment. i, Fluorescence under 514 nm. ii, Fluorescence under 488 nm. iii, Bright-field image. No significant GFP fluorescence was observed when the *wrky33* protoplasts were transfected with P_{ACS2}:*GUS-GFP* or P_{ACS6}:*GUS-GFP*, even on GSH treatment. However, when the *wrky33* protoplasts were cotransfected with $P_{CaMV35S}$:*YFP-WRKY33* and P_{ACS2}:*GUS-GFP* or P_{ACS6}:*GUS-GFP* constructs, significant GFP fluorescence was observed, and fluorescence level increased on GSH treatment. YFP fluorescence indicated the constitutive WRKY33 expression. Experiments were performed in replicates of three. Bar = 10 μm.

S-glutathionylated proteins followed by western blot against anti-ACO1 antibody revealed that this protein is a target for *S*-glutathionylation. However, we could not detect ACS2 and ACS6 proteins among the *S*-glutathionylated proteins (Fig. 12).

Homology Modeling and Docking Analysis Revealed ACO1 Is *S*-Glutathionylated on CYS63 Residue

Because Arabidopsis ACO1 (AtACO1) shared a high level of amino acid identity with petunia (*Petunia hybrida*) ACO (PhACO), homology modeling (or comparative protein structure modeling) could be applied to generate the three-dimensional conformation of AtACO1. A restraint-based program, MODELER 9v1 (Sali and Blundell, 1993), was used for generating the three-dimensional model of AtACO1. For model building, the program MODELER 9v1 was used with the pdb coordinates of 1W9Y chain A and 1WA6 chain X (crystal structure of *Petunia* × *hybrid* ACO; Zhang et al., 2004) as templates (Fig. 13, A and B). The model of lowest energy value had 94.7% residues in the most favored regions in the Ramachandran plot, and 85.36% residues had an average three-dimensional-one-dimensional score above 0.2, as obtained through VERIFY3D profile, which affirms a well-derived model (Supplemental Fig. S11, A and B).

Literature review suggests that two relevant factors in protein susceptibility for *S*-glutathionylation are steric accessibility of the Cys residues and its vicinity to side chains of basic amino acids (Demasi et al., 2014). Analysis of the three-dimensional structure of AtACO1 revealed that the CYS63 residue is sterically accessible, and surface topography analysis by CASTp server revealed a binding pocket surrounding this residue

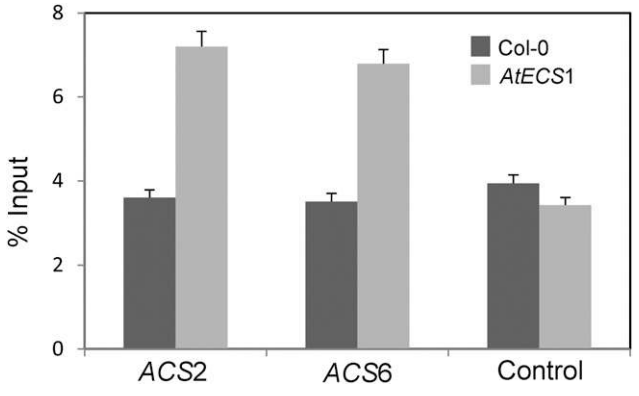

Figure 10. Analysis of association of WRKY33 with promoters of *ACS2* and *ACS6* under altered GSH conditions. ChIP assay revealed an enhanced association of WRKY33 to both the promoters in *AtECS1* (higher GSH content) than Col-0. Input percentage indicates fold enrichment. Association of RNA polymerase II with GAPDH promoter was used as control.

(Supplemental Fig. S11C). This residue also has His and Lys residues in its vicinity, thus making it a possible target for *S*-glutathionylation. Molecular docking analysis revealed that GSH can bind CYS63 residue of AtACO1 protein, and the distance between sulfur atoms of GSH and CYS63 is 2.6 Å (Fig. 13, C and D), which is comparable with the 2.10-Å distance of the crystal structure of glutathionylated yeast (*Saccharomyces cerevisiae*) Glutaredoxin1 protein (Yu et al., 2008). Together, our observation suggests that ACO1 is a subject for *S*-glutathionylation on the CYS63 residue.

GSH-ET Interplay Plays Crucial Role in Regulating Stress Tolerance

Defense against necrotrophic infection by *B. cinerea* as well as salt stress is known to occur through ET-mediated pathway (Díaz et al., 2002; Cao et al., 2007). Hence, we selected these two stresses to assess the biological significance of GSH-ET interplay during stress. The *AtECS1* plants exhibited increased resistance to both the stresses, while GSH-depleted *pad2-1* mutant was sensitive (Fig. 14, A and B). Transcript analysis revealed a stronger induction of *ACS2*, *ACS6*, and *ACO1* genes in *AtECS1* during infection as well as salt stress, while a weaker induction was observed in *pad2-1* mutant. GSH and ACC levels were also higher in *AtECS1* and lower in *pad2-1* during stress compared with Col-0 (Fig. 14, C and D). These observations signify a key role of GSH in imparting stress tolerance in plants. To check if the GSH-mediated resistance is dependent on ET, we studied the stress response of Col-0 and the ET-signaling mutant *ethylene insensitive2-1* (*ein2-1*) with and without exogenously fed GSH. We observed that exogenously applied GSH could improve stress tolerance in Col-0 but not in *ein2-1* plants (Fig. 15). Together, our results indicate that GSH-mediated resistance to necrotrophic infection and salt stress occurs in an ET-dependent fashion.

DISCUSSION

Plants are continuously challenged by numerous biotic and abiotic stress factors. GSH has been known to play a crucial role in modulating plant defense response for more than a couple of decades (Dron et al., 1988; Wingate et al., 1988). It is one of the central players in stress management through its interaction with different established signaling molecules. It has been reported that GSH confers biotic stress tolerance in plants through NPR1-dependent SA-mediated pathway (Ghanta et al., 2011a). Subsequently, GSH has also been reported to act independent of NPR1 to increase intracellular hydrogen peroxide, which activates SA signaling (Han et al., 2013). We have recently reported the crosstalk of GSH with ET, in addition to SA, to combat environmental stress in planta (Ghanta et al., 2014). However, the mechanism of GSH-ET interplay is still unexplored. In this investigation, we demonstrate that GSH induces ET biosynthesis by modulating transcriptional as well as posttranscriptional regulations. The proposed model for this GSH-ET interplay has been summarized in Figure 16.

The enzyme γ-ECS catalyzes the key step in GSH biosynthesis (Hell and Bergmann, 1990; May et al., 1998). Overexpressing this enzyme in *AtECS* lines successfully enhanced the GSH contents up to 2.24-fold. On the other hand, a mutated *γ-ECS* gene in *pad2-1* mutant has reduced the GSH content to approximately 22% of that of the wild type (Parisy et al., 2007). Hence, comparing the *AtECS1* with enhanced GSH level and the GSH-depleted *pad2-1* mutant can reveal valuable information. In plants, defense against necrotrophic infection by *B. cinerea* occurs via an ET-mediated signaling pathway (Díaz et al., 2002). In addition, ET is also involved in imparting tolerance against several abiotic stresses, including salt stress (Cao et al., 2007). In this study, the enhanced resistance of *AtECS1* line to *B. cinerea* infection as well as salt stress demonstrated the role of GSH in defense against these stress conditions. Depletion of GSH, on the other hand, led to severe susceptibility of the *pad2-1* plants to both the stresses. Exogenously applied GSH could also improve the stress tolerance potential in Col-0 plants, supporting further the involvement of GSH in defense against these two stresses. However, resistance could not be enhanced by exogenous GSH in the ET-signaling mutant *ein2-1*, thus suggesting that this GSH-mediated stress tolerance is dependent on the ET-responsive pathway.

ET synthesis is a two-step process where the first step is catalyzed by ACS while the final step is catalyzed by ACO enzyme. Transcript analysis revealed stronger induction of *ACS* and *ACO* genes in response to stress in *AtECS1* and weaker induction in *pad2-1* mutant. Even the ET and ACC levels were higher under enhanced GSH conditions. Together, our observations indicate that GSH-mediated tolerance against these stresses occurs by induction of ET pathway. In addition, ET is known to induce petiole hyponasty

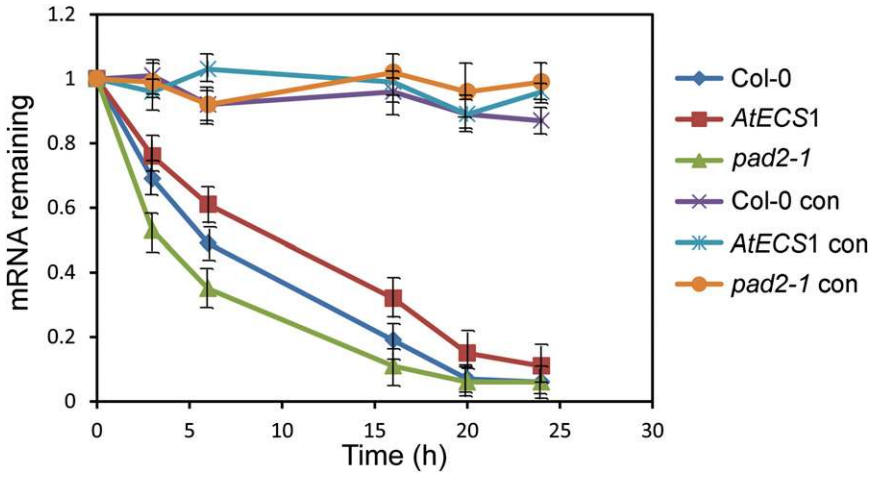

Figure 11. Analysis of mRNA stability of *ACO1* under altered GSH conditions. Col-0, *AtECS1*, and *pad2-1* seedlings were treated with actinomycin D on a temporal landscape followed by qRT-PCR analysis. Control seedlings were treated with water. The mRNA stability was found to be increased in *AtECS1* and decreased in *pad2-1* compared with Col-0. Data are the mean ± SD for three individual experiments using plants treated independently.

in plants (Polko et al., 2011). Hence, the petiole hyponasty observed in the *AtECS* lines is indicative of the higher ET level in the transgenic lines, which is a possible effect of the enhanced GSH content. To study the effect of altered GSH levels on cellular protein, we performed a comparative proteomic analysis of *AtECS1*, Col-0, and *pad2-1* leaves. The elevated GSH level in *AtECS1* led to up-regulation of ACO protein, while it was down-regulated in the GSH-depleted *pad2-1*. Together with the stress response, ACC levels under stress and the accumulation of ACO protein in *AtECS1* and *pad2-1*, it is convincible that GSH induces ET synthesis by modulating the key biosynthetic enzymes.

It is worth mentioning here that ACS is encoded by a small gene family in all plant species. In Arabidopsis, there are nine ACS members, which can be grouped as type I, type II, and type III (Han et al., 2010). Type I isoforms include *ACS2* and *ACS6* isoforms and account for 80% of the ET synthesized during stress (Li et al., 2012). Type II isoforms include *ACS4*, *ACS5*, *ACS8*, and *ACS9*, while type III includes *ACS7* and *ACS11*. The ACS isoforms have been reported to display cell- or tissue-specific expression, and some members are highly responsive to extracellular stimuli (Wang et al., 2002; Tsuchisaka and Theologis, 2004). In addition, posttranslational modifications of ACS members by protein phosphorylation plays a critical role in determining cellular ACS activity and ET production (Liu and Zhang, 2004; Wang et al., 2004; Chae and Kieber, 2005; Joo et al., 2008). Nevertheless, ET synthesis is a highly complex phenomenon regulated at multiple levels. Consequently, many details of its regulation still remain unknown, including the regulatory pathways that control expression of *ACS* genes and the stability of the gene products (Han et al., 2010). It would be interesting to note that, in this study, only the ACS2 and ACS6 isoforms were up-regulated in transcript as well as protein levels in *AtECS1* while down-regulated in *pad2-1*. The rest of the isoforms were unaffected. In case of the ACO enzyme, only ACO1 expression was affected. In addition, exogenously fed GSH could also augment the expression of ACS2, ACS6, and ACO1 but not the other isoforms. Depleting the GSH content in Col-0 plants by BSO feeding also affected only the above-mentioned isoforms, thus supporting the fact that GSH-mediated induction of ET synthesis is isoform specific.

GSH is a nearly ubiquitous molecule and is involved in regulating diverse physiological processes, ranging from developmental aspects to various stress responses. Consequently, GSH-mediated regulation of genes and proteins is a complex process occurring at multiple levels. GSH-mediated induction of ACS and ACO enzymes can occur at several possible levels. First, GSH can induce *ACS* and *ACO* expression at transcript level via modulation of transcriptional regulator(s). The change in cellular redox homeostasis, a consequence of elevated GSH level under stress, can be the second possible way for modulating ACS and ACO expression levels. The third point of regulation can be modulation of mRNA stability of the target genes. Fourth, post-translational modification of ACS and ACO proteins by

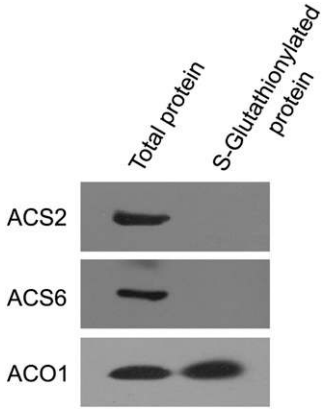

Figure 12. Analysis of *S*-glutathionylation of ACS and ACO proteins. Western-blot analysis was performed from total and in vitro *S*-glutathionylated proteins against anti-ACS2, anti-ACS6, and anti-ACO1 antibodies. Only the *S*-glutathionylation of ACO1 protein was detected.

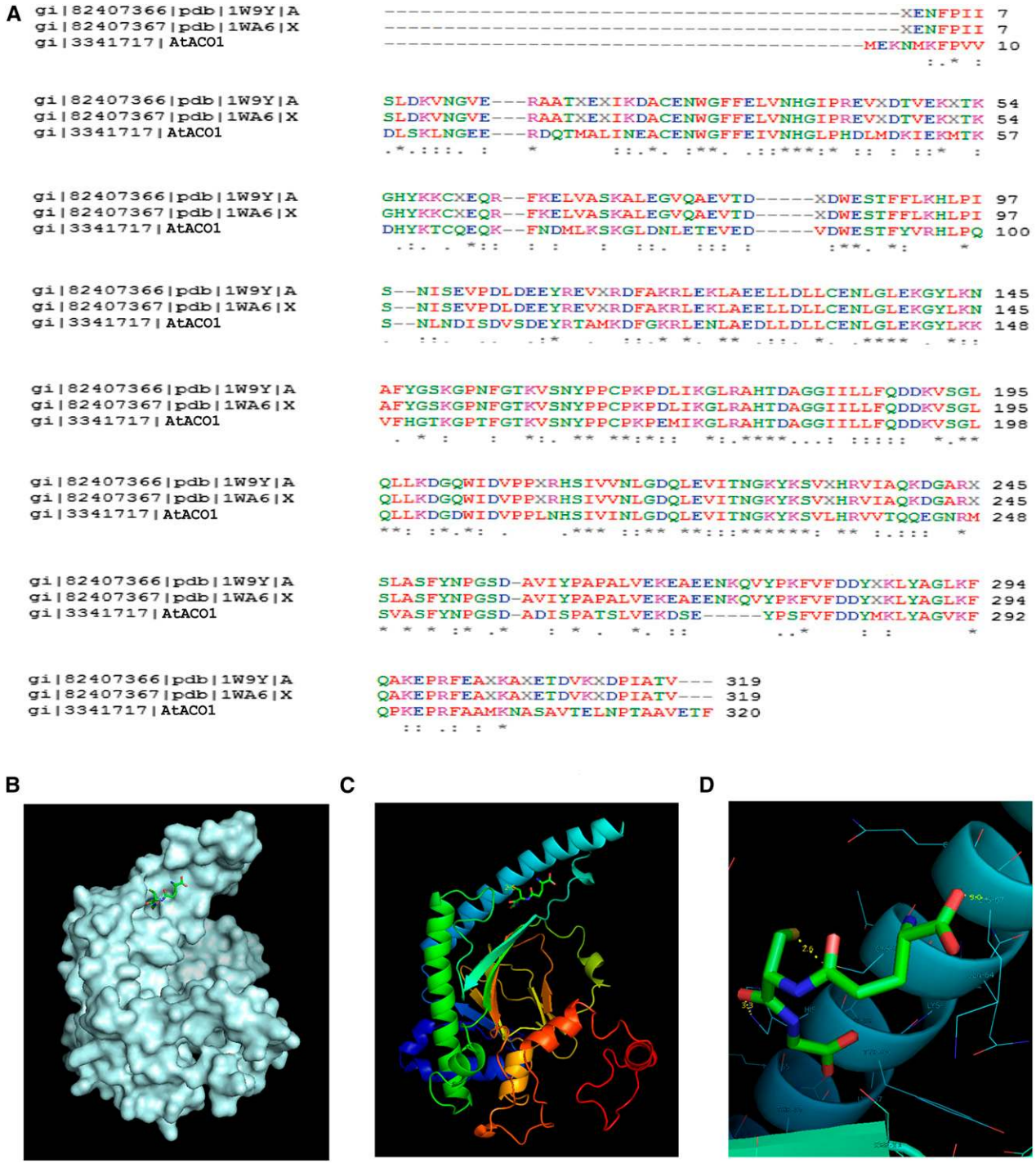

Figure 13. In silico prediction of the site for *S*-glutathionylation in AtACO1 protein. A, Protein sequence alignment of AtACO1 with PhACO (1W9Y|A and 1WA6|X). B, Molecular surface view of the homology model of AtACO1 protein docked with GSH. Model building was based on PhACO structure. C, Ribbon diagram of the same. D, Close view of the binding site of GSH.

S-glutathionylation can be another option to regulate protein stability/activity. Thus, it would be worthy to explore each of these possibilities to decipher the mechanism by which GSH induces ACS and ACO and augments ET synthesis.

Our promoter analysis result demonstrated that higher GSH level could elevate the promoter activity of *ACS2* and *ACS6*, while it did not affect the *ACO1* promoter. Furthermore, a positive feedback induction of all the three promoters by ET was observed, which can be

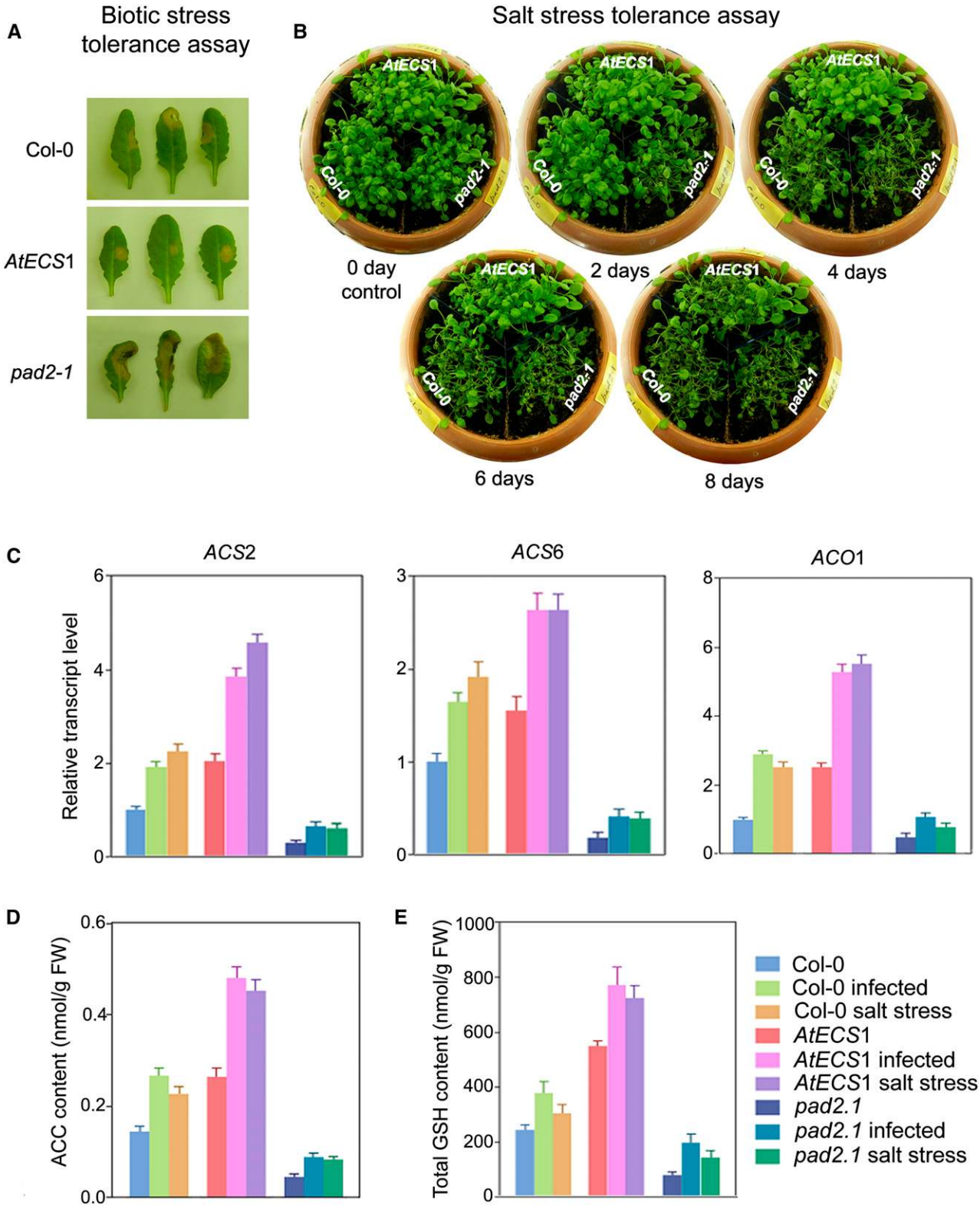

Figure 14. Stress response assay of Col-0, *AtECS1*, and *pad2-1* plants. A, Biotic stress assay in response to *B. cinerea* infection. B, Abiotic stress assay in response to salt stress. The *AtECS1* plants exhibited resistance against both the stresses, while the *pad2-1* mutant was susceptible. C, qRT-PCR analysis of *ACS2*, *ACS6*, and *ACO1* genes in Col-0, *AtECS1*, and *pad2-1* in response to stress. Estimation of ACC content (D) and total GSH content (E) in Col-0, *AtECS1*, and *pad2-1* in response to stress. Data are the mean ± SD for three individual experiments using plants grown independently. FW, Fresh weight.

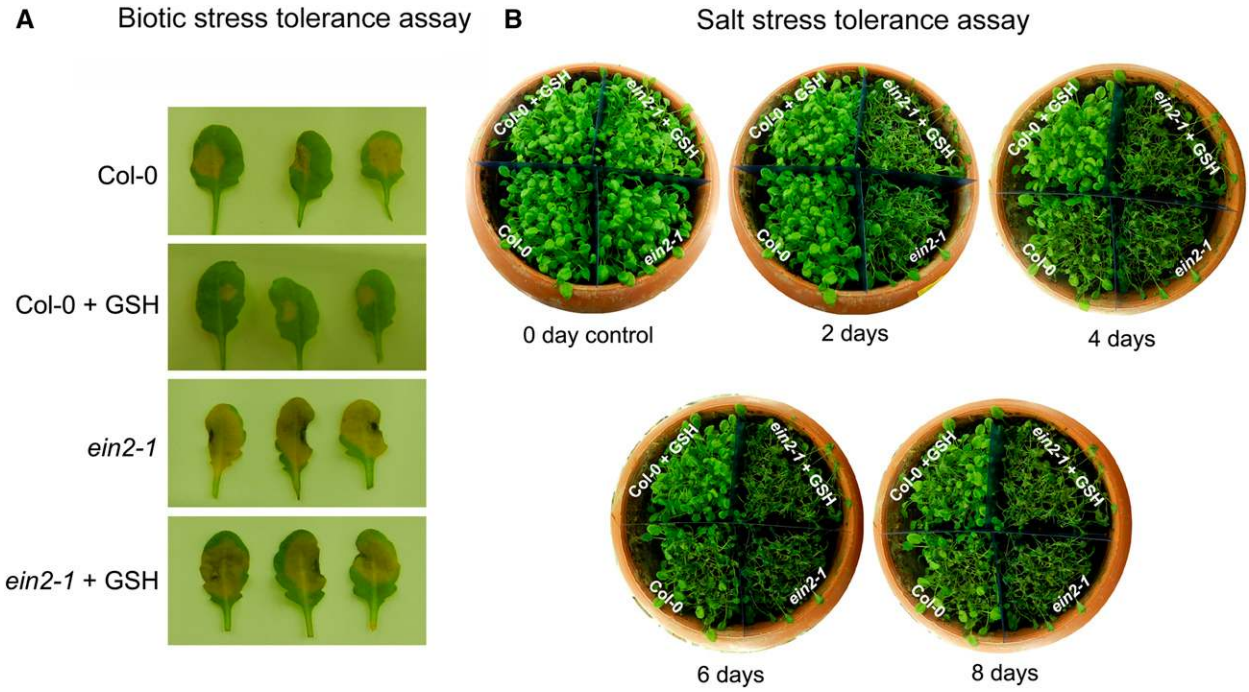

Figure 15. Stress response assay of Col-0 and *ein2-1* plants with and without GSH feeding. A, Biotic stress assay in response to *B. cinerea* infection. B, Abiotic stress assay in response to salt stress. GSH feeding improved stress tolerance in Col-0 plants but not in *ein2-1* mutant. All experiments were repeated three times.

corroborated with previous reports (Wang et al., 2004). Because GSH cannot directly bind to the promoter for transcriptional induction, it becomes necessary to identify the pathway or the transcriptional regulator through which GSH modulates the promoter activity. MPK cascades are signaling pathways downstream of sensors/receptors that transduce extracellular stimuli into intracellular responses in eukaryotes. In plants, ET

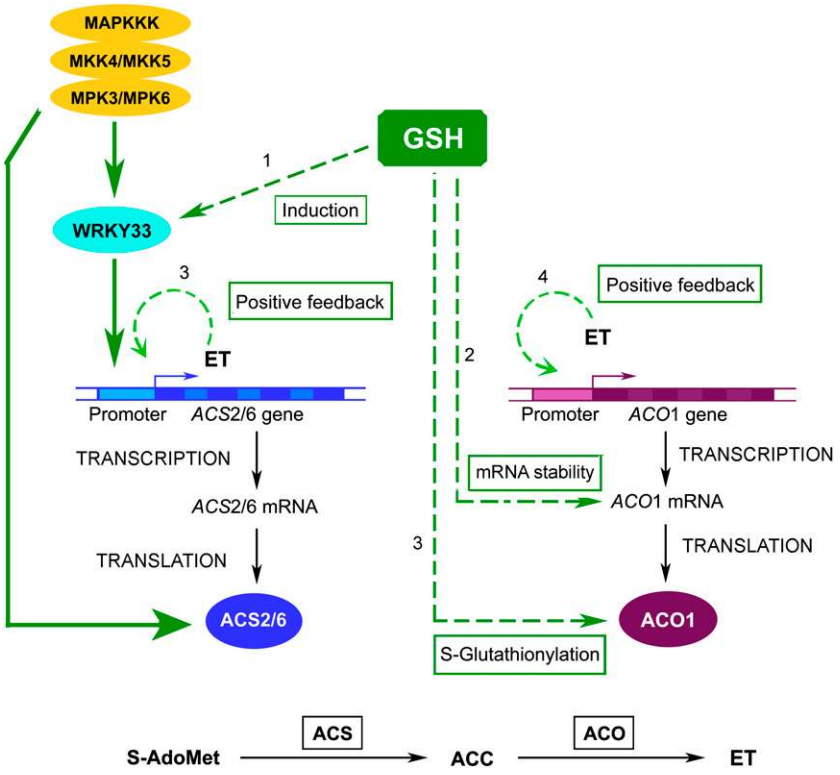

Figure 16. Proposed model for regulation of ET biosynthesis by GSH. 1, GSH induces *ACS2* and *ACS6* transcription in a WRKY33-dependent manner during stress. This increases the transcript levels of *ACS2* and *ACS6*. Consequently, more ACS2 and ACS6 proteins are synthesized. 2, On the other hand, GSH enhances the stability of the ACO1 mRNA, and consequently more ACO1 protein is synthesized. 3, In addition, *S*-glutathionylation of ACO1 protein is also detected. Together, this leads to increased synthesis of ET. 4, Increased ET level then enhances *ACS2*, *ACS6*, and *ACO1* transcription via positive feedback induction, thus further augmenting the ET production. Dashed arrow indicates proposed regulation. Solid arrow indicates established regulation. MAPKKK, Mitogen-activated protein kinase kinase kinase.

production is induced by a subset of MPKs, represented by MPK3/MPK6, during various stress conditions (Tena et al., 2001; Zhang and Klessig, 2001; Ichimura et al., 2002; Jonak et al., 2002). ACS2 and ACS6 proteins are substrates of MPK3 and MPK6 (Liu and Zhang, 2004; Han et al., 2010). Phosphorylation of ACS2/ACS6 by MPK6/MPK3 stabilizes the ACS protein in vivo, resulting in an increase in cellular ACS activity and ET production (Joo et al., 2008). The transcriptional regulation of ACS2 and ACS6 during stress also occurs via the MKK4/MKK5/MKK9-MPK3/MPK6-WRKY33 pathway (Li et al., 2012). However, in this study, we observed that GSH-mediated induction of *ACS2* and *ACS6* was not affected in *mpk3* and *mpk6* mutants, indicating that this regulation is independent of MPK3/MPK6 pathway. Consequently, there must be some alternative pathways that function in regulating *ACS2* and *ACS6* transcription during stress, even when the MPK3/MPK6 pathway is blocked. Several transcription factors are involved in regulating *ACS2* and *ACS6* expression under various conditions. Among them WRKY33 is an important regulator during necrotrophic infection and functions downstream of MKK4/MKK5/MKK9-MPK3/MPK6 pathway (Li et al., 2012). Our mutant analysis revealed that the GSH-mediated induction of *ACS2* and *ACS6* transcription does not occur in *wrky33* mutant, indicating a critical involvement of this transcription factor in GSH-mediated defense. Cotransfection assay of the *ACS2* or *ACS6* promoters with *WRKY*33 in the *wrky33* protoplast reconfirmed the above observation. Together, it appears likely that, under stress, the cellular GSH content rises, which may increase the binding of WRKY33 to *ACS2* and *ACS6* promoters, leading to increased expression of these genes.

Because changes in the steady-state levels of mRNA can result from regulation of either transcription or mRNA degradation, we sought to explore the mRNA stability of *ACO1* under altered GSH conditions. Interestingly, our observations revealed that the mRNA stability was considerably enhanced in *AtECS1* and reduced in *pad2-1* compared with the wild type, thus demonstrating a significant role of GSH in modulating the mRNA stability of the *ACO1* gene.

S-glutathionylation is the formation of mixed disulphide bonds between GSH and Cys residues of proteins. Originally, *S*-glutathionylation was thought to be a result of oxidative stress (Ziegler, 1985). Later on, it became recognized as a posttranslational modification that can play major regulatory functions (Gallogly and Mieyal, 2007; Dalle-Donne et al., 2009; Hill and Bhatnagar, 2012). Because the intracellular environment is highly reducing, very few protein thiols are actually prone to be *S*-glutathionylated, and the process occurs in a site- and protein-specific manner (Demasi et al., 2014). Here, we could identify that ACO1 protein is *S*-glutathionylated, while *S*-glutathionylation of ACS2 and ACS6 was not detected. Our in silico analysis further revealed that the *S*-glutathionylation presumably occurs on the CYS63 residue of the AtACO1 protein. This observation can be corroborated with a previous report, which states that ACO is a probable target of *S*-glutathionylation (Dixon et al., 2005).

CONCLUSION

In this investigation, the molecular mechanism of GSH-ET interplay under environmental stress conditions has been elucidated. GSH positively modulates ACS2, ACS6, and ACO1 expression, thus augmenting ET biosynthesis. We further revealed that for *ACS2* and *ACS6*, GSH regulates gene expression by WRKY33-mediated transcriptional induction. On the other hand, it modulates the mRNA stability of the *ACO1* gene, thus enhancing the steady-state mRNA levels in the cell. In addition, we could detect that the ACO1 protein was a subject for *S*-glutathionylation on its CYS63 residue. Together, the current study reveals the molecular mechanism of ET-GSH crosstalk during stress.

MATERIALS AND METHODS

Plant Material and Growth Condition

Arabidopsis (*Arabidopsis thaliana*) Col-0 served as the wild type. The *pad2-1* mutant carries a mutation in the γ-*ECS* gene and contains only approximately 22% of the wild-type amount of GSH (Parisy et al., 2007). The *ein2-1* mutant is an ET-signaling mutant where the *EIN2* gene is mutated (Alonso et al., 1999). Seeds for Col-0, *pad2-1*, and *ein2-1* mutants were procured from the Nottingham Arabidopsis Stock Centre. Plants were grown in Murashige and Skoog (MS) media and maintained in a growth chamber at 22°C under 16-h-light/8-h-dark cycles as standardized before until stated otherwise (Datta et al., 2013).

Raising of Transgenic Arabidopsis Overexpressing γ-*ECS* Gene

The coding region of γ-*ECS* gene from *Lycopersicum esculentum* was cloned into pBI121 plasmid under *CaMV35S* promoter (Ghanta et al., 2011a) and introduced into Col-0 plants via *Agrobacterium tumefaciens*-mediated transformation following floral dip method (Clough and Bent, 1998). T1 seeds were harvested, dried at 25°C, and germinated on sterile MS medium containing 40 mg L^{-1} kanamycin to select the transformants. Surviving T1 plantlets were transferred to soil to set T2 seeds. The lines were chosen based on their transgene expression as well as vigor. Independent homozygous lines (*AtECS*) were selected and maintained up to T4 generation.

Genomic DNA was extracted from leaves of *AtECS* lines by cetyl trimethyl ammonium bromide method. PCR was employed to screen the transformants carrying *npt*II and *Le-*γ*-ECS* gene. A list of primers used is presented in Supplemental Table S3.

Southern-Blot Analysis of *AtECS* Lines

For Southern-blot analysis, a total of 10 μg of genomic DNA was digested with *Eco*RI and *Hin*dIII separately, fractionated on 0.8% (w/v) agarose gel, and then transferred onto Immobilon-NY$^+$ membrane (Millipore). Hybridization was performed at 68°C using a 700-bp fragment of *Le-*γ*-ECS* as probe labeled with [α-^{32}P] dATP. The blots were washed repeatedly under stringent conditions and exposed to x-ray film (Sambrook and Russell, 2001; Ghanta et al., 2011a).

qRT-PCR Analysis

Total RNA was extracted leaf samples using the Trizol method. Complementary DNA was synthesized using the RevertAid HMinus cDNA Synthesis Kit (Fermentas). The qRT-PCR was performed using Light Cycler 96 System

(Roche Applied Science) with FastStart Essential DNA Green Master (Roche Applied Science). qRT-PCR was performed for selected genes with primer pairs listed in Supplemental Table S3. The constitutively expressed *actin* gene was used as the reference gene.

Western-Blot Analysis

Proteins were extracted after homogenizing leaves in 50 mM potassium phosphate buffer, pH 7.8, containing 0.15% (v/v) Triton X-100. Protein samples were quantified by Bradford assay (Bradford, 1976) using bovine serum albumin as standard, resolved in 12% (w/v) SDS-PAGE gel, transferred onto polyvinylidene difluoride membrane (Millipore), and blocked with 5% (w/v) skimmed milk. The γ-ECS protein bands were detected by using a rabbit polyclonal anti-γ-ECS antibody as the primary antibody and an anti-rabbit IgG conjugated to horseradish peroxidase as the secondary antibody (Agrisera). For detecting ACS2, ACS6, and ACO1 proteins, goat polyclonal anti-ACS2, anti-ACS6, and anti-ACO1 antibodies (Santa Cruz Biotechnology) were used as the primary antibody and an anti-goat IgG conjugated to horseradish peroxidase as the secondary antibody. Immunoreactive proteins were visualized using the SuperSignal West Pico chemiluminescent substrate (Pierce).

Estimation of Total GSH Content and GSH:GSSG Ratio

GSH was extracted from leaves and quantified (Tsakraklides et al., 2002). HPLC was conducted using a 515-HPLC pump (Waters) and 2475 fluorescence detector (Waters) at a flow rate of 1.5 mL min^{-1} using AccQ.Tag (3.9 × 9 × 150 mm) column (Waters) at an excitation wavelength of 360 nm and emission wavelength of 450 nm. Briefly, the elution condition was solvent A, composed of sodium acetate and triethylamine at pH 5.05 at 5% (v/v) dilution, and acetonitrile:water (30:70) as solvent B. From 0 to 9 min, A was 94% (v/v), from 9 to 16 min, a linear gradient of 94% to 91.5% (v/v) A was applied, from 16 to 22 min, a linear gradient of 75% (v/v) A was applied, and from 22 to 30 min, A decreased to 0% (v/v) linearly. GSH (Sigma) was used as standard. Data analyses were performed with Empower 2 software.

The GSH:GSSG ratio was measured according to Ishikawa et al. (2010) as standardized before (Ghanta et al., 2011a).

Estimation of ACC Content

Estimation of ACC was performed by *o*-phthaldialdehyde precolumn derivatization method (Bushey et al., 1987). The HPLC analysis was conducted using a 515 HPLC pump with a 2475 fluorescence detector as mentioned above at a flow rate of 0.6 mL min^{-1}. AccQ-Tag (3.9 × 9 × 150 mm) column with an excitation wavelength of 325 nm and an emission wavelength of 465 nm was used. The elution condition was solvent A, composed of 0.1 M sodium acetate at pH 5.8, and methanol as solvent B. Initially, B was 10% (v/v). From 0 to 4 min, a linear gradient of 10% to 44% (v/v) B was applied, from 4 to 10 min, a linear gradient of 44% to 50% (v/v) B was applied, from 10 to 12 min, a linear gradient of 50% to 80% (v/v) B was applied, from 12 to 16 min, 80% to 100% (v/v) B, and from 16 to 20 min, B decreased to 0% (v/v) linearly.

Estimation of ET Level

ET estimation was performed according to Vogel et al. (1998). Briefly, plant samples were incubated in 22-mL gas chromatography vials containing 3 mL of MS medium at 21°C for 24 h. Appropriate supplements as indicated were included in the media. The vials were flushed with hydrocarbon-free air and then capped. The accumulated ET was measured by using a gas chromatograph (Agilent Technologies) fitted with a PoraPLOT U column, a cryofocusing attachment, and a flame ionization detector. A sample of headspace from each sample was injected with an autosampler onto the column, and the column was then warmed to 30°C. The ET peaks were quantified based on comparison to a 1 μL L^{-1} ET standard. All observations were from at least three replicates.

Chemical Treatment of Seedlings

Two-week-old seedlings were used for all feeding experiments. For GSH and BSO feeding, seedlings were fed separately with 100 μM GSH and 1 mM BSO solutions for 24-, 48-, 72-, and 96-h GSH solutions as standardized before (Sinha et al., 2014). Feeding was monitored by estimating GSH content of GSH-fed seedlings by HPLC analysis. A 72-h feeding was found to be optimum for both cases. For DTT feeding, seedlings were fed with 5 mM freshly prepared DTT solution, and feeding was monitored using *PR1* gene expression (Gomez et al., 2004). For ascorbate feeding, 20 mM solution was used and monitored by estimating ascorbate content in fed seedlings (Huang et al., 2005). Maximum ascorbate accumulation occurred after 12 h of feeding. Estimation of ascorbate content was performed following Kampfenkel et al. (1995). For Eth treatment, a 50 μM aqueous solution was used (Stotz et al., 2000).

Promoter Analysis

To clone the promoter regions of *ACS2*, *ASC6*, and *ACO1* genes, approximately 1.5 kb of intergenic region upstream of the transcription start site was cloned into pCAMBIA1303 plasmid with the *GUS* (*uidA*) gene under control of these promoters. The resulting constructs were P_{ACS2}:*GUS*, P_{ACS6}:*GUS*, and P_{ACO1}:*GUS*, respectively. These constructs were transformed into Col-0 plants following *A. tumefaciens*-mediated floral dip method as described above (Clough and Bent, 1998). The resulting transgenic lines were denoted as *pACS2*, *pACS6*, and *pACO1*, respectively.

Histochemical GUS staining of control and GSH- and Eth-fed seedlings of *pACS2*, *pACS6*, and *pACO1* were performed as described previously (Tateda et al., 2011). Plant samples were treated with cold 90% (v/v) acetone for 15 min on ice and washed twice with 100 mM phosphate buffer (pH 7.0). The samples were soaked in GUS staining solution (0.5 mg mL^{-1} 5-bromo-4-chloro-3-indolyl-β-glucuronic acid, 0.5 mM potassium ferrocyanide, 0.5 mM potassium ferricyanide, 0.1% [v/v] Triton X-100, 100 mM phosphate buffer, pH 7.0, and 10 mM EDTA) and subjected to weak negative pressure using a vacuum pump. The samples were further incubated in the same solution for 16 h, fixed in 70% (v/v) ethanol, and then observed by light microscopy.

Protoplast Transfection Assay

Protoplasts isolation and transfection were performed according to Yoo et al. (2007). Briefly, protoplasts were isolated from the leaves of 3-week-old Col-0 and *AtECS1* plants and were transfected with the P_{ACS2}:*GUS-GFP*, P_{ACS6}:*GUS-GFP*, and P_{ACO1}:*GUS-GFP* constructs separately via polyethylene glycol-$CaCl_2$ method. After transfection, the protoplasts were maintained for 5 h at room temperature. The GFP expression levels in Col-0 and *AtECS1* protoplasts for each construct were visualized under confocal laser scanning microscope.

Protoplast Cotransfection Assay

The *WRKY33* coding sequence was cloned from Arabidopsis complementary DNA in the pAM-PAT-YFP vector under the control of the *CaMV35S* constitutive promoter. The resulting construct was $P_{CaMV35S}$:*YFP-WRKY33*. Next, protoplasts were isolated from the leaves of 3-week-old *wrky33* mutant. The *wrky33* protoplasts were similarly transfected with $P_{CaMV35S}$:*YFP-WRKY33*, P_{ACS2}:*GUS-GFP*, or P_{ACS6}:*GUS-GFP*. Next, the construct $P_{CaMV35S}$:*YFP-WRKY33* was cotransfected with P_{ACS2}:*GUS-GFP* or P_{ACS6}:*GUS-GFP* in the *wrky33* protoplasts via polyethylene glycol-$CaCl_2$ method. For GSH feeding of the cotransfected protoplasts, GSH was added to the protoplast maintenance medium to a final concentration of 100 μM after the transfection event and maintained for 5 h at room temperature. The GFP and YFP expression levels were visualized under confocal laser scanning microscope.

ChIP-qPCR Assay

Leaves of 15-d-old Col-0 and *AtECS* plants were used for ChIP analysis. Anti-WRKY33 antibody (Ab-mart) was used to pull down the chromatin, as described previously (Jin et al., 2008; Yoo et al., 2010). Leaves were incubated in buffer (0.4 M Suc, 10 mM Tris, pH 8.0, 1 mM EDTA, 1 mM phenylmethylsulfonyl fluoride, and 1% [v/v] formaldehyde) under vacuum for 15 min to crosslink the chromatin. Then, 0.1 M Gly was added to the mixture, which was incubated for an additional 5 min to terminate the reaction. Leaves were ground in liquid nitrogen and resuspended in 1× phosphate-buffered saline. The assay was performed using EZ-ChIP kit (Millipore) following manufacturer's protocol. Binding of RNA polymerase II to GAPDH promoter was used as control. The primers used are listed in Supplemental Table S3. Three independent experiments were performed with similar results. Data are mean values of three replicates ± SD.

mRNA Stability Assay

Col-0, *AtECS*, and *pad2-1* plants were harvested under water and incubated for 0, 2, 6, 12, 18, and 24 h in 200 mM actinomycin D (Sigma-Aldrich). Prior to this

treatment, plants were preincubated in actinomycin D for 30 min to allow proper distribution of the antibiotic. Plants incubated with water served as a control. Total RNA was isolated, and qRT-PCR analysis was performed for *ACO1* gene.

In Vitro *S*-Glutathionylation Analysis

Col-0 cell cultures (50 mL) were maintained, used, and harvested in midlog growth as described (Loutre et al., 2003). In vitro *S*-glutathionylation analysis was performed according to Dixon et al. (2005). Briefly, Col-0 cells (10 g) were homogenized in 0.1 M Tris-Cl, pH 7.5, containing 1 mM EDTA and 2 mM DTT and, after centrifugation (13,000*g* for 20 min), protein precipitated by addition of $(NH_4)_2SO_4$ to 80% (w/v) saturation. Following recentrifugation, the protein pellet was desalted in 20 mM Tris-Cl, pH 7.5 (18 mL), using a HiTrap desalting column (Amersham Biosciences). GSSG-biotin (10 μM) was added to the sample and incubated for 10 min, prior to precipitation of the proteins with 80% (w/v) $(NH_4)_2SO_4$. The pellet was then washed with buffer A (20 mM Tris-Cl, 0.5 M NaCl, and 1 mM EDTA, pH 6.8) containing 80% (w/v) $(NH_4)_2SO_4$, to remove unreacted GSSG-biotin, prior to desalting the protein in buffer A (12 mL). For in vitro thiolation, protein was extracted in 0.1 M Tris-Cl, pH 7.5, containing 1 mM EDTA and then treated as above, except that the initial desalting GSSG-biotin treatment and subsequent precipitation steps were omitted. To purify thiolated proteins, 750 μL of streptavidin-agarose resin (Amersham Biosciences), prewashed with buffer A, was added to the extract and mixed gently for 10 min. The matrix was pelleted by centrifugation (700*g* for 2 min) and washed four times with 40 mL of buffer A. The matrix was then resuspended in buffer A (4 mL) containing 10 mM DTT for 15 min at 20°C to release proteins that had formed mixed disulfides with biotinylated GSH. The filtered protein extract was precipitated with acetone (16 mL) at −20°C for 16 h, and the pellet was washed with 80% (v/v) acetone. As a control, the above was repeated using nonbiotinylated GSSG to detect proteins that bound nonspecifically to the streptavidin matrix. After binding the thiolated protein mixture, the matrix was treated with 2.5 mL of buffer B (20 mM Tris-Cl and 6 M urea, pH 6.8). Following 15-min incubation at 20°C, the displaced protein solution was separated from the matrix by filtration, with the streptavidin-agarose resin, and then washed two times with 25 mL of buffer A, and the disulfide-bound protein was recovered with buffer A containing DTT. To detect whether ACS2, ACS6, and ACO1 proteins are targets of *S*-glutathionylation, western-blot analysis was performed with the isolated pool of *S*-glutathionylated proteins against anti-ACS2, anti-ACS6, and anti-ACO1 antibodies.

Homology Modeling and Molecular Docking

A restraint-based program MODELER 9v1 (Sali and Blundell, 1993) was used for generating the three-dimensional model of AtACO1. Initially, the AtACO1 amino acid sequence was allowed to search for potentially related sequences. The AtACO1 sequence was aligned with the corresponding template, and the three-dimensional model was calculated based on the lowest value of MODELER objective function (Sali and Blundell, 1993). The resulting model was subjected to PROCHECK (Laskowski et al., 1993) and VERIFY3D (Lüthy et al., 1992) to evaluate the model folding and the stereochemistry. Energy minimization was performed using the Yasara server.

As the volume of the active-site groove influences the binding of the substrate molecule, the active-site groove volume of the enzyme was measured through CASTp calculation (Dundas et al., 2006). The docking experiment was performed using AutoDock Vina (Trott and Olson, 2010). The initial coordinates of the ligand (GSH) were obtained from the PRODRG server. AutoDock Tools (Morris et al., 2009) was used to prepare the ligand and receptor (AtACO1 and GSH) PDBQT files to include charges and hydrogen atoms. AutoDock Vina was then used for docking the ligand into a search box ($30 \times 30 \times 30$ Å^3) centered near the active-site groove around CYS63 residue.

Stress Assay

Disease test with *Botrytis cinerea* was performed according to a previous report with minor modifications (Ferrari et al., 2003). Briefly, the fungus was grown for 14 d in petri dishes containing potato dextrose agar at 25°C in the dark. Inoculation with *B. cinerea* was conducted by placing four 5-μL droplets of a spore suspension potato dextrose broth on each leaf (two fully expanded leaves per plant). Inoculated plants were covered with a transparent plastic dome to maintain high humidity. Parallel controls were inoculated with potato dextrose broth. After 5 d, disease progression was checked and photographed.

For salt stress, 2-week-old plants grown in soil were watered every alternate day with 200 mM NaCl solution for 8 d. Plants were monitored every day and photographed. For GSH feeding, the plants were watered with 10 mL of 100 μM GSH solution every day until harvested.

Supplemental Data

The following supplemental materials are available.

Supplemental Figure S1. Southern-blot analysis of *AtECS* lines.

Supplemental Figure S2. Comparative proteome analysis of Col-0, *AtECS1*, and *pad2-1*.

Supplemental Figure S3. ET level was estimated from leaves of 2-week-old GSH-fed Col-0 plants.

Supplemental Figure S4. Effect of DTT and β-mercaptoethanol feeding on gene expression.

Supplemental Figure S5. Effect of altered GSH levels on the expression of *MPK3*, *MPK6*, *MKK4*, *MKK5*, and *MKK9* genes.

Supplemental Figure S6. Expression profile of *ACO1* gene in *mpk3*, *mpk6*, *wrky6*, *wrky8*, *wrky33*, *erf4*, and *erf11* mutants.

Supplemental Figure S7. Analysis of association of WRKY33 with promoters of *ACS2* and *ACS6* under altered GSH conditions.

Supplemental Figure S8. Estimation of ascorbate content in Col-0, *AtECS1*, *AtECS19*, *AtECS23*, *AtECS25*, and *pad2-1* plants.

Supplemental Figure S9. Effect of GSH and ascorbate feeding on ACO1 in *pad2-1*.

Supplemental Figure S10. Analysis of mRNA stability of *ACO1* under altered GSH conditions.

Supplemental Figure S11. Analysis of homology model of AtACO1.

Supplemental Table S1. Differentially expressed proteins in the leaf proteome of *AtECS1* in comparison to Col-0 as identified by MALDI-TOF-MS/MS.

Supplemental Table S2. Differentially expressed proteins in the leaf proteome of *pad2-1* in comparison to Col-0 as identified by MALDI-TOF-MS/MS.

Supplemental Table S3. List of primers used.

ACKNOWLEDGMENTS

We thank the central proteomics facility of the Council of Scientific and Industrial Research-Indian Institute of Chemical Biology and Sudip Chattopadhyay (National Institute of Technology, Durgapur) for sharing the *A. tumefaciens* GV3103 strain and the pAM-PAT-YFP vector with us.

Received October 1, 2015; accepted October 8, 2015; published October 13, 2015.

LITERATURE CITED

Abeles FB, Morgan PW, Saltveit ME (1992) Ethylene in plant biology. Ed 2. Academic Press, San Diego

Achard P, Cheng H, De Grauwe L, Decat J, Schoutteten H, Moritz T, Van Der Straeten D, Peng J, Harberd NP (2006) Integration of plant responses to environmentally activated phytohormonal signals. Science **311:** 91–94

Alonso JM, Hirayama T, Roman G, Nourizadeh S, Ecker JR (1999) EIN2, a bifunctional transducer of ethylene and stress responses in Arabidopsis. Science **284:** 2148–2152

Ball L, Accotto GP, Bechtold U, Creissen G, Funck D, Jimenez A, Kular B, Leyland N, Mejia-Carranza J, Reynolds H, et al (2004) Evidence for a direct link between glutathione biosynthesis and stress defense gene expression in *Arabidopsis*. Plant Cell **16:** 2448–2462

Bell AA (1981) Biochemical mechanisms of disease resistance. Annu Rev Plant Physiol **32:** 21–81

Bradford MM (1976) A rapid and sensitive method for the quantitation of microgram quantities of protein utilizing the principle of protein-dye binding. Anal Biochem **72:** 248–254

Bradley DJ, Kjellbom P, Lamb CJ (1992) Elicitor- and wound-induced oxidative cross-linking of a proline-rich plant cell wall protein: a novel, rapid defense response. Cell **70:** 21–30

Bushey DF, Law DM, Davies PJ (1987) High-performance liquid chromatography analysis of 1-aminocyclopropane-1-carboxylic acid using o-phthaldialdehyde precolumn derivatization. Anal Biochem **167:** 31–36

Cao WH, Liu J, He XJ, Mu RL, Zhou HL, Chen SY, Zhang JS (2007) Modulation of ethylene responses affects plant salt-stress responses. Plant Physiol **143:** 707–719

Chae HS, Kieber JJ (2005) Eto Brute? Role of ACS turnover in regulating ethylene biosynthesis. Trends Plant Sci **10:** 291–296

Chagué V, Danit LV, Siewers V, Schulze-Gronover C, Tudzynski P, Tudzynski B, Sharon A (2006) Ethylene sensing and gene activation in *Botrytis cinerea*: a missing link in ethylene regulation of fungus-plant interactions? Mol Plant Microbe Interact **19:** 33–42

Chappell J, Hahlbrock K, Boller T (1984) Rapid induction of ethylene biosynthesis in cultured parsley cells by fungal elicitor and its relationship to the induction of phenylalanine ammonia-lyase. Planta **161:** 475–480

Chen YF, Etheridge N, Schaller GE (2005) Ethylene signal transduction. Ann Bot (Lond) **95:** 901–915

Cheng MC, Liao PM, Kuo WW, Lin TP (2013) The Arabidopsis ETHYLENE RESPONSE FACTOR1 regulates abiotic stress-responsive gene expression by binding to different cis-acting elements in response to different stress signals. Plant Physiol **162:** 1566–1582

Clough SJ, Bent AF (1998) Floral dip: a simplified method for *Agrobacterium*-mediated transformation of *Arabidopsis thaliana*. Plant J **16:** 735–743

Dalle-Donne I, Rossi R, Colombo G, Giustarini D, Milzani A (2009) Protein *S*-glutathionylation: a regulatory device from bacteria to humans. Trends Biochem Sci **34:** 85–96

Datta R, Chattopadhyay S (2015) Changes in the proteome of *pad2-1*, a glutathione depleted Arabidopsis mutant, during *Pseudomonas syringae* infection. J Proteomics **126:** 82–93

Datta R, Sinha R, Chattopadhyay S (2013) Changes in leaf proteome profile of *Arabidopsis thaliana* in response to salicylic acid. J Biosci **38:** 317–328

Demasi M, Netto LES, Silva GM, Hand A, de Oliveira CLP, Bicev RN, Gozzo F, Barros MH, Leme JMM, Ohara E (2014) Redox regulation of the proteasome via *S*-glutathionylation. Redox Biol **2:** 44–51

Díaz J, ten Have A, van Kan JAL (2002) The role of ethylene and wound signaling in resistance of tomato to *Botrytis cinerea*. Plant Physiol **129:** 1341–1351

Dixon DP, Skipsey M, Grundy NM, Edwards R (2005) Stress-induced protein *S*-glutathionylation in Arabidopsis. Plant Physiol **138:** 2233–2244

Dong X (1998) SA, JA, ethylene, and disease resistance in plants. Curr Opin Plant Biol **1:** 316–323

Dron M, Clouse SD, Dixon RA, Lawton MA, Lamb CJ (1988) Glutathione and fungal elicitor regulation of a plant defense gene promoter in electroporated protoplasts. Proc Natl Acad Sci USA **85:** 6738–6742

Dundas J, Ouyang Z, Tseng J, Binkowski A, Turpaz Y, Liang J (2006) CASTp: computed atlas of surface topography of proteins with structural and topographical mapping of functionally annotated residues. Nucleic Acids Res **34:** W116–W118

Elad Y (1990) Production of ethylene by tissues of tomato, pepper, French-bean and cucumber in response to infection by *Botrytis cinerea*. Physiol Mol Plant Pathol **36:** 277–287

Esquerré-Tugayé MT, Lafitte C, Mazau D, Toppan A, Touzé A (1979) Cell surfaces in plant-microorganism interactions. Plant Physiol **64:** 320–326

Etheridge N, Chen YF, Schaller GE (2005) Dissecting the ethylene pathway of Arabidopsis. Brief Funct Genomics Proteomics **3:** 372–381

Fan X, Mattheis JP, Roberts RG (2000) Biosynthesis of phytoalexin in carrot root requires ethylene action. Physiol Plant **110:** 450–454

Ferrari S, Plotnikova JM, De Lorenzo G, Ausubel FM (2003) Arabidopsis local resistance to *Botrytis cinerea* involves salicylic acid and camalexin and requires EDS4 and PAD2, but not SID2, EDS5 or PAD4. Plant J **35:** 193–205

Foyer CH, Noctor G (2011) Ascorbate and glutathione: the heart of the redox hub. Plant Physiol **155:** 2–18

Gallogly MM, Mieyal JJ (2007) Mechanisms of reversible protein glutathionylation in redox signaling and oxidative stress. Curr Opin Pharmacol **7:** 381–391

Ghanta S, Bhattacharyya D, Chattopadhyay S (2011b) Glutathione signaling acts through NPR1-dependent SA-mediated pathway to mitigate biotic stress. Plant Signal Behav **6:** 607–609

Ghanta S, Bhattacharyya D, Sinha R, Banerjee A, Chattopadhyay S (2011a) *Nicotiana tabacum* overexpressing γ-ECS exhibits biotic stress tolerance likely through NPR1-dependent salicylic acid-mediated pathway. Planta **233:** 895–910

Ghanta S, Chattopadhyay S (2011) Glutathione as a signaling molecule: another challenge to pathogens. Plant Signal Behav **6:** 783–788

Ghanta S, Datta R, Bhattacharyya D, Sinha R, Kumar D, Hazra S, Mazumdar AB, Chattopadhyay S (2014) Multistep involvement of glutathione with salicylic acid and ethylene to combat environmental stress. J Plant Physiol **171:** 940–950

Glazebrook J (2005) Contrasting mechanisms of defense against biotrophic and necrotrophic pathogens. Annu Rev Phytopathol **43:** 205–227

Glazebrook J, Ausubel FM (1994) Isolation of phytoalexin-deficient mutants of *Arabidopsis thaliana* and characterization of their interactions with bacterial pathogens. Proc Natl Acad Sci USA **91:** 8955–8959

Gomez LD, Noctor G, Knight MR, Foyer CH (2004) Regulation of calcium signalling and gene expression by glutathione. J Exp Bot **55:** 1851–1859

Gullner G, Kömives T, Rennenberg H (2001) Enhanced tolerance of transgenic poplar plants overexpressing gamma-glutamylcysteine synthetase towards chloroacetanilide herbicides. J Exp Bot **52:** 971–979

Habben JE, Bao X, Bate NJ, DeBruin JL, Dolan D, Hasegawa D, Helentjaris TG, Lafitte RH, Lovan N, Mo H, et al (2014) Transgenic alteration of ethylene biosynthesis increases grain yield in maize under field drought-stress conditions. Plant Biotechnol J **12:** 685–693

Han L, Li GJ, Yang KY, Mao G, Wang R, Liu Y, Zhang S (2010) Mitogen-activated protein kinase 3 and 6 regulate *Botrytis cinerea*-induced ethylene production in Arabidopsis. Plant J **64:** 114–127

Han Y, Chaouch S, Mhamdi A, Queval G, Zechmann B, Noctor G (2013) Functional analysis of Arabidopsis mutants points to novel roles for glutathione in coupling H_2O_2 to activation of salicylic acid accumulation and signaling. Antioxid Redox Signal **18:** 2106–2121

Hell R, Bergmann L (1990) λ-Glutamylcysteine synthetase in higher plants: catalytic properties and subcellular localization. Planta **180:** 603–612

Hill BG, Bhatnagar A (2012) Protein *S*-glutathiolation: redox-sensitive regulation of protein function. J Mol Cell Cardiol **52:** 559–567

Hoffman T, Schmidt JS, Zheng X, Bent AF (1999) Isolation of ethylene-insensitive soybean mutants that are altered in pathogen susceptibility and gene-for-gene disease resistance. Plant Physiol **119:** 935–950

Howden R, Andersen CR, Goldsbrough PB, Cobbett CS (1995) A cadmium-sensitive, glutathione-deficient mutant of *Arabidopsis thaliana*. Plant Physiol **107:** 1067–1073

Huang C, He W, Guo J, Chang X, Su P, Zhang L (2005) Increased sensitivity to salt stress in an ascorbate-deficient Arabidopsis mutant. J Exp Bot **56:** 3041–3049

Ishikawa K, Yoshimura K, Harada K, Fukusaki E, Ogawa T, Tamoi M, Shigeoka S (2010) AtNUDX6, an ADP-ribose/NADH pyrophosphohydrolase in Arabidopsis, positively regulates NPR1-dependent salicylic acid signaling. Plant Physiol **152:** 2000–2012

Jin JB, Jin YH, Lee J, Miura K, Yoo CY, Kim WY, Van Oosten M, Hyun Y, Somers DE, Lee I, et al (2008) The SUMO E3 ligase, *AtSIZ1*, regulates flowering by controlling a salicylic acid-mediated floral promotion pathway and through affects on *FLC* chromatin structure. Plant J **53:** 530–540

Jonak C, Okrész L, Bögre L, Hirt H (2002) Complexity, cross talk and integration of plant MAP kinase signalling. Curr Opin Plant Biol **5:** 415–424

Joo S, Liu Y, Lueth A, Zhang S (2008) MAPK phosphorylation-induced stabilization of ACS6 protein is mediated by the non-catalytic C-terminal domain, which also contains the cis-determinant for rapid degradation by the 26S proteasome pathway. Plant J **54:** 129–140

Kampfenkel K, Van Montagu M, Inzé D (1995) Extraction and determination of ascorbate and dehydroascorbate from plant tissue. Anal Biochem **225:** 165–167

Ichimura K, Shinozaki K, Tena G, Sheen J, Henry Y, Champion A, Kreis M, Zhang S, Hirt H (2002) Mitogen-activated protein kinase cascades in plants: a new nomenclature. Trends Plant Sci **7:** 301–308

Knoester M, van Loon LC, van den Heuvel J, Hennig J, Bol JF, Linthorst HJM (1998) Ethylene-insensitive tobacco lacks nonhost resistance against soil-borne fungi. Proc Natl Acad Sci USA **95:** 1933–1937

Kunkel BN, Brooks DM (2002) Cross talk between signaling pathways in pathogen defense. Curr Opin Plant Biol **5:** 325–331

Larkindale J, Knight MR (2002) Protection against heat stress-induced oxidative damage in Arabidopsis involves calcium, abscisic acid, ethylene, and salicylic acid. Plant Physiol **128:** 682–695

Laskowski RA, MacArthur MW, Moss DS, Thornton JM (1993) PROCHECK: a program to check the stereochemical quality of protein structures. J Appl Cryst **26:** 283–291

Li G, Meng X, Wang R, Mao G, Han L, Liu Y, Zhang S (2012) Dual-level regulation of ACC synthase activity by MPK3/MPK6 cascade and its downstream WRKY transcription factor during ethylene induction in Arabidopsis. PLoS Genet **8:** e1002767

Liedschulte V, Wachter A, Zhigang A, Rausch T (2010) Exploiting plants for glutathione (GSH) production: Uncoupling GSH synthesis from cellular controls results in unprecedented GSH accumulation. Plant Biotechnol J **8:** 807–820

Liu Y, Zhang S (2004) Phosphorylation of 1-aminocyclopropane-1-carboxylic acid synthase by MPK6, a stress-responsive mitogen-activated protein kinase, induces ethylene biosynthesis in *Arabidopsis*. Plant Cell **16:** 3386–3399

Loake G, Grant M (2007) Salicylic acid in plant defence: the players and protagonists. Curr Opin Plant Biol **10:** 466–472

Loutre C, Dixon DP, Brazier M, Slater M, Cole DJ, Edwards R (2003) Isolation of a glucosyltransferase from *Arabidopsis thaliana* active in the metabolism of the persistent pollutant 3,4-dichloroaniline. Plant J **34:** 485–493

Lüthy R, Bowie JU, Eisenberg D (1992) Assessment of protein models with three-dimensional profiles. Nature **356:** 83–85

Manavella PA, Arce AL, Dezar CA, Bitton F, Renou JP, Crespi M, Chan RL (2006) Cross-talk between ethylene and drought signalling pathways is mediated by the sunflower Hahb-4 transcription factor. Plant J **48:** 125–137

Marte M, Buonaurio R, Della Torre G (1993) Induction of systemic resistance to tobacco powdery mildew by tobacco mosaic virus, tobacco necrosis virus or ethephon. J Phytopathol **138:** 137–144

May MJ, Vernoux T, Leaver C, Montagu MV, Inzé D (1998) Glutathione homeostasis in plants: implications for environmental sensing and plant development. J Exp Bot **49:** 649–667

Meister A (1988) Glutathione metabolism and its selective modification. J Biol Chem **263:** 17205–17208

Morris GM, Huey R, Lindstrom W, Sanner MF, Belew RK, Goodsell DS, Olson AJ (2009) AutoDock4 and AutoDockTools4: automated docking with selective receptor flexibility. J Comput Chem **30:** 2785–2791

Mou Z, Fan W, Dong X (2003) Inducers of plant systemic acquired resistance regulate NPR1 function through redox changes. Cell **113:** 935–944

Mullineaux PM, Rausch T (2005) Glutathione, photosynthesis and the redox regulation of stress-responsive gene expression. Photosynth Res **86:** 459–474

Noctor G, Arisi ACM, Jouanin L, Foyer CH (1998) Manipulation of glutathione and amino acid biosynthesis in the chloroplast. Plant Physiol **118:** 471–482

Noctor G, Mhamdi A, Chaouch S, Han Y, Neukermans J, Marquez-Garcia B, Queval G, Foyer CH (2012) Glutathione in plants: an integrated overview. Plant Cell Environ **35:** 454–484

O'Donnell PJ, Calvert C, Atzorn R, Wasternack C, Leyser HMO, Bowles DJ (1996) Ethylene as a signal mediating the wound response of tomato plants. Science **274:** 1914–1917

O'Donnell PJ, Schmelz E, Block A, Miersch O, Wasternack C, Jones JB, Klee HJ (2003) Multiple hormones act sequentially to mediate a susceptible tomato pathogen defense response. Plant Physiol **133:** 1181–1189

Parisy V, Poinssot B, Owsianowski L, Buchala A, Glazebrook J, Mauch F (2007) Identification of *PAD2* as a γ-glutamylcysteine synthetase highlights the importance of glutathione in disease resistance of Arabidopsis. Plant J **49:** 159–172

Penninckx IAMA, Thomma BPHJ, Buchala A, Métraux JP, Broekaert WF (1998) Concomitant activation of jasmonate and ethylene response pathways is required for induction of a plant defensin gene in *Arabidopsis*. Plant Cell **10:** 2103–2113

Pieterse CMJ, Dicke M (2007) Plant interactions with microbes and insects: from molecular mechanisms to ecology. Trends Plant Sci **12:** 564–569

Polko JK, Voesenek LACJ, Peeters AJM, Pierik R (2011) Petiole hyponasty: an ethylene-driven, adaptive response to changes in the environment. AoB Plants **2011:** plr031

Reymond P, Farmer EE (1998) Jasmonate and salicylate as global signals for defense gene expression. Curr Opin Plant Biol **1:** 404–411

Sali A, Blundell TL (1993) Comparative protein modelling by satisfaction of spatial restraints. J Mol Biol **234:** 779–815

Sambrook J, Russell DW (2001) Molecular Cloning: A Laboratory Manual. CSHL Press, Cold Spring Harbor, NY

Schlaeppi K, Bodenhausen N, Buchala A, Mauch F, Reymond P (2008) The glutathione-deficient mutant *pad2-1* accumulates lower amounts of glucosinolates and is more susceptible to the insect herbivore *Spodoptera littoralis*. Plant J **55:** 774–786

Shakeel SN, Wang X, Binder BM, Schaller GE (2013) Mechanisms of signal transduction by ethylene: overlapping and non-overlapping signalling roles in a receptor family. AoB Plants **5:** plt010

Sinha R, Kumar D, Datta R, Hazra S, Bhattacharyya D, Mazumdar AB, Mukhopadhyay R, Sultana A, Chattopadhyay S (2014) Integrated transcriptomic and proteomic analysis of *Arabidopsis thaliana* exposed to glutathione unravels its role in plant defense. Plant Cell Tissue Organ Cult **120:** 975–988

Stotz HU, Pittendrigh BR, Kroymann J, Weniger K, Fritsche J, Bauke A, Mitchell-Olds T (2000) Induced plant defense responses against chewing insects. Ethylene signaling reduces resistance of Arabidopsis against Egyptian cotton worm but not diamondback moth. Plant Physiol **124:** 1007–1018

Stout MJ, Thaler JS, Thomma BPHJ (2006) Plant-mediated interactions between pathogenic microorganisms and herbivorous arthropods. Annu Rev Entomol **51:** 663–689

Tateda C, Watanabe K, Kusano T, Takahashi Y (2011) Molecular and genetic characterization of the gene family encoding the voltage-dependent anion channel in Arabidopsis. J Exp Bot **62:** 4773–4785

Tena G, Asai T, Chiu WL, Sheen J (2001) Plant mitogen-activated protein kinase signaling cascades. Curr Opin Plant Biol **4:** 392–400

Thomma BPHJ, Eggermont K, Penninckx IAMA, Mauch-Mani B, Vogelsang R, Cammue BPA, Broekaert WF (1998) Separate jasmonate-dependent and salicylate-dependent defense-response pathways in Arabidopsis are essential for resistance to distinct microbial pathogens. Proc Natl Acad Sci USA **95:** 15107–15111

Trott O, Olson AJ (2010) AutoDock Vina: improving the speed and accuracy of docking with a new scoring function, efficient optimization, and multithreading. J Comput Chem **31:** 455–461

Tsakraklides G, Martin M, Chalam R, Tarczynski MC, Schmidt A, Leustek T (2002) Sulfate reduction is increased in transgenic *Arabidopsis thaliana* expressing 5′-adenylylsulfate reductase from *Pseudomonas aeruginosa*. Plant J **32:** 879–889

Tsuchisaka A, Theologis A (2004) Unique and overlapping expression patterns among the Arabidopsis 1-amino-cyclopropane-1-carboxylate synthase gene family members. Plant Physiol **136:** 2982–3000

van Loon LC, Geraats BPJ, Linthorst HJM (2006) Ethylene as a modulator of disease resistance in plants. Trends Plant Sci **11:** 184–191

Vernoux T, Wilson RC, Seeley KA, Reichheld JP, Muroy S, Brown S, Maughan SC, Cobbett CS, Van Montagu M, Inzé D, et al (2000) The *ROOT MERISTEMLESS1/CADMIUM SENSITIVE2* gene defines a glutathione-dependent pathway involved in initiation and maintenance of cell division during postembryonic root development. Plant Cell **12:** 97–110

Vogel JP, Woeste KE, Theologis A, Kieber JJ (1998) Recessive and dominant mutations in the ethylene biosynthetic gene *ACS5* of Arabidopsis confer cytokinin insensitivity and ethylene overproduction, respectively. Proc Natl Acad Sci USA **95:** 4766–4771

Wang KLC, Li H, Ecker JR (2002) Ethylene biosynthesis and signaling networks. Plant Cell **14**(Suppl) **:** S131–S151

Wang KLC, Yoshida H, Lurin C, Ecker JR (2004) Regulation of ethylene gas biosynthesis by the Arabidopsis ETO1 protein. Nature **428:** 945–950

Wingate VP, Lawton MA, Lamb CJ (1988) Glutathione causes a massive and selective induction of plant defense genes. Plant Physiol **87:** 206–210

Xiang C, Werner BL, Christensen EM, Oliver DJ (2001) The biological functions of glutathione revisited in Arabidopsis transgenic plants with altered glutathione levels. Plant Physiol **126:** 564–574

Yoo CY, Pence HE, Jin JB, Miura K, Gosney MJ, Hasegawa PM, Mickelbart MV (2010) The *Arabidopsis* GTL1 transcription factor regulates water use efficiency and drought tolerance by modulating stomatal density via transrepression of *SDD1*. Plant Cell **22:** 4128–4141

Yoo SD, Cho YH, Sheen J (2007) Arabidopsis mesophyll protoplasts: a versatile cell system for transient gene expression analysis. Nat Protoc **2:** 1565–1572

Yu J, Zhang NN, Yin PD, Cui PX, Zhou CZ (2008) Glutathionylation-triggered conformational changes of glutaredoxin Grx1 from the yeast *Saccharomyces cerevisiae*. Proteins **72:** 1077–1083

Zhang S, Klessig DF (2001) MAPK cascades in plant defense signaling. Trends Plant Sci **6:** 520–527

Zhang Z, Ren JS, Clifton IJ, Schofield CJ (2004) Crystal structure and mechanistic implications of 1-aminocyclopropane-1-carboxylic acid oxidase: the ethylene-forming enzyme. Chem Biol **11:** 1383–1394

Zhu YL, Pilon-Smits EAH, Tarun AS, Weber SU, Jouanin L, Terry N (1999) Cadmium tolerance and accumulation in Indian mustard is enhanced by overexpressing γ-glutamylcysteine synthetase. Plant Physiol **121:** 1169–1178

Ziegler DM (1985) Role of reversible oxidation-reduction of enzyme thiols-disulfides in metabolic regulation. Annu Rev Biochem **54:** 305–329